JOURNAL OF MORPHOLOGY 277:957–977 (2016)

# A Comparative Ultrastructural Analysis of Spermatozoa in *Pleurodema* (Anura, Leptodactylidae, Leiuperinae)

**Julio C. Cruz,[1,2] Daiana P. Ferraro,[3,4] Alejandro Farías,[1] Julio S. Santos,[5] Shirlei M. Recco-Pimentel,[5] Julián Faivovich,[4] and Gladys N. Hermida[1]***

[1]*Laboratorio Biología de Anfibios, Histología Animal, Departamento de Biodiversidad y Biología Experimental, Facultad de Ciencias Exactas y Naturales, Universidad de Buenos Aires, Ciudad Autónoma de Buenos Aires, Argentina*
[2]*Instituto de Bio y Geociencias (IBIGEO) - CONICET, Universidad de Salta, Salta, Argentina*
[3]*Instituto Nacional de Limnología (INALI) - CONICET, Santa Fe, Argentina*
[4]*División Herpetología, Museo Argentino de Ciencias Naturales "Bernardino Rivadavia" - CONICET, Ciudad Autónoma de Buenos Aires, Argentina*
[5]*Departamento de Biologia Estrutural e Funcional, Instituto de Biologia, Universidade Estadual de Campinas (UNICAMP), Brazil*

*ABSTRACT* This study describes the spermatozoa of 10 of the 15 species of the Neotropical frog genus *Pleurodema* through transmission electron microscopy. The diversity of oviposition modes coupled with a recent phylogenetic hypothesis of *Pleurodema* makes it an interesting group for the study of ultrastructural sperm evolution in relation to fertilization environment and egg-clutch structure. We found that *Pleurodema* has an unusual variability in sperm morphology. The more variable structures were the acrosomal complex, the midpiece, and the tail. The acrosomal complex has all the structures commonly reported in hyloid frogs but with different degree of development of the subacrosomal cone. Regarding the midpiece, the variability is given by the presence or absence of the mitochondrial collar. Finally, the tail is the most variable structure, ranging from single (only axoneme) to more complex (presence of paraxonemal rod, cytoplasmic sheath, and undulating membrane), with the absence of the typical axial fiber present in hyloid frogs, also shared with some other genera of Leiuperinae. J. Morphol. 277:957–977, 2016. 

KEY WORDS: ultrastructure; phylogeny; foam nest; spermatozoon

## INTRODUCTION

The Neotropical Leiuperinae (*sensu* Pyron and Wiens, 2011 with modifications by Faivovich et al., 2012) currently includes about 90 species (Frost, 2015) distributed in five genera, *Edalorhina*, *Engystomops*, *Physalaemus*, *Pleurodema*, and *Pseudopaludicola*. The monophyly of Leiuperinae is supported by molecular evidence (Pyron and Wiens, 2011). In this clade, the ancestral condition of the egg-clutch structure is egg-laying on foam nest on water, as occurs in all the species of *Edalorhina*, *Engystomops*, and *Physalaemus* for which reproductive mode is known (see Faivovich et al., 2012 and literature therein). While species of *Pseudopaludicola* lay eggs individually on water (Barrio, 1954; Giaretta and Facure, 2009), *Pleurodema* exhibits a striking variability.

The genus *Pleurodema*, distributed from Panama to southern South America, encompasses 15 species (Faivovich et al., 2012). Three different egg-clutch structures were described for the genus: eggs laid in floating foam nests, eggs included in gelatinous strings (floating or submerged), and eggs laid in gelatinous subspherical masses that result from the collapse of the foam nest subsequent to the spawning process (Cei, 1962, 1980; Barrio, 1964, 1977; Duellman and Veloso, 1977; Hödl, 1992; Martori et al., 1994; Weigandt et al., 2004; Ferraro et al., 2016).

The ultrastructure of anuran spermatozoa has been associated with phylogenetic relationships and with fertilization environment (Jamieson et al., 1993; Lee and Jamieson, 1993). It has been postulated that a complex spermatozoon as observed in basal lineages of anurans, caecilians, and salamanders is the plesiomorphic condition in amphibians. This spermatozoon, characterized by the presence of both accessory fibers and undulating membrane, was also related to internal fertilization and/or viscous fertilization environments

*Correspondence to: Gladys N. Hermida, Laboratorio Biología de Anfibios, Histología Animal, Departamento de Biodiversidad y Biología Experimental, 4° Piso, Pab II, Facultad de Ciencias Exactas y Naturales, Universidad de Buenos Aires, Av. Int. Güiraldes 2620, Ciudad Universitaria (C1428EHA), Ciudad Autónoma de Buenos Aires, Argentina. E-mail: gladyshermida@gmail.com

Received 13 October 2015; Revised 10 March 2016;
Accepted 5 April 2016.

Published online 6 May 2016 in
Wiley Online Library (wileyonlinelibrary.com).
DOI 10.1002/jmor.20550

(Jamieson et al., 1993; Lee and Jamieson, 1993). A simpler spermatozoon has been associated with aquatic fertilization environments (Jamieson et al., 1993; Lee and Jamieson, 1993; Scheltinga et al., 2002a; Scheltinga and Jamieson, 2003; Garda et al., 2004). In Rhacophoridae, where the fertilization takes place in foam nests, neither accessory fibers nor an undulating membrane are present, but a packed core of satellite microtubules is observed surrounding the double axoneme (Mainoya, 1981; Mizuhira et al., 1986; Muto and Kubota, 2009, 2013). Recently, Muto and Kubota (2009, 2013) studied two foam-nesting Rhacophorids and suggested that the sperm motility is specifically modified for a viscous fertilization environment. Within Rhacophoridae, members of the genera *Chiromantis*, *Polypedates*, and *Rhacophorus* share common character states, a pair of axonemes surrounded by hundreds of crystallized satellite microtubules in the tail of the spermatozoa. These features provide more propulsion power and flagellar stiffness, which opposes the viscous resistance of the foam nest and generates higher bending torque (Muto and Kubota, 2013). Furthermore, spermatozoa of non foam-nesting Rhacophoridae (e.g., *Burgeria buergeri*) do not have these complex features (Muto and Kubota, 2013).

The ultrastructure of spermatozoa has been described in eighteen species of Leiuperinae: *Engystomops pustulosus* (as *Physalaemus pustulosus*, Scheltinga, 2002), *Physalaemus biligonigerus*, *P. gracilis*, *P. marmoratus* (as *P. fuscomaculatus*, Amaral et al., 1999), *P. nattereri* (as *Eupemphix nattereri*, Zieri et al., 2008), *Pleurodema thaul* (Pugin and Garrido, 1981), *Pseudopaludicola falcipes* (Amaral et al., 2000), and *Pseudopaludicola ameghini*, *P. atragula*, *P. canga*, *P. facureae*, *P. giarettai*, *P. mineira*, *P. mystacalis*, *P. saltica*, *P. ternetzi*, *Pseudopaludicola* sp. 1, and *Pseudopaludicola* sp. 2 (Santos et al., 2015).

The diversity of oviposition modes in *Pleurodema*, coupled with a recent phylogenetic hypothesis, makes this group an interesting candidate for the study of ultrastructural sperm evolution in relation with fertilization environment and egg-clutch structure.

The goals of this contribution were i) to describe the spermatozoon ultrastructure of ten species of *Pleurodema* and ii) to establish hypotheses of homology involving the ultrastructure of spermatozoids and to study its evolution in the phylogenetic context of Leiuperinae. Finally, we discussed the relationship between spermatozoon ultrastructure and reproductive modes in foam nesting species in general, and in *Pleurodema* in particular.

## MATERIALS AND METHODS

The testes of ten species of *Pleurodema* were examined (see Appendix). Samples were obtained from adult males housed at herpetological collections (*Pleurodema borellii*, *P. brachyops*, *P. bufoninum, P. cinereum*, and *P. marmoratum* from CENAI collection) or recently collected (*P. cordobae*, *P. diplolister*, *P. guayapae, P. kriegi*, *P. marmoratum* from LGE collection, and *P. tucumanum*). These latter specimens were sacrificed by immersion in a 10% aqueous solution of tricaine methanesulfonate (MS-222). The testes were quickly removed and cut into small fragments (1 $mm^3$) in 0.1 M sodium phosphate buffer (pH 7.2) and fixed for transmission electron microscopy (TEM) in 3% glutaraldehyde in 0.1 M sodium phosphate buffer (pH 7.2) at 4°C overnight.

Specimens from herpetological collections were fixed in 10% formalin and stored in 70% ethanol. The testes of these specimens were rehydrated through a descending ethanol series following the methodology by Scheltinga et al. (2002b). Subsequently, they were placed into 3% glutaraldehyde in 0.1 M sodium phosphate buffer (pH 7.2) at 4°C overnight, before processing and sectioning as for normal glutaraldehyde-fixed tissues (described below).

All samples were rinsed in 0.1 M sodium phosphate buffer; postfixed for 1 h in 1% osmium tetroxide in the same buffer; dehydrated through an ascending ethanol series; and embedded in epoxy resin and polymerized. Semithin sections were cut at 2 μm and stained with 1% toluidine blue in $Na_2CO_3$. Ultrathin sections were cut at 90–150 nm with a glass blade on a Sorvall Porter Blum MT2-B Ultra-Microtome (Ivan Sorvall Inc., Newtown, CT), and stained with uranyl acetate and lead citrate (Reynolds, 1963). Electron micrographs were taken using a Philips EM 301 transmission electron microscope at 75–80 kV and a Zeiss EM 109T at 75 kV equipped with a Gatan ES1000W digital camera (11 megapixels). The electron micrographs with the best definition of structures were selected for analysis (e.g., chromatin with compacted material and absence of residual cytoplasmic material derived from cyto differentiation).

Based on the informative variation observed in the ultrastuctural sperm morphology, homology hypotheses were defined and optimized on the phylogenetic hypothesis of *Pleurodema* proposed by Faivovich et al. (2012). Characters were scored based on photographs of transverse sections of spermatozoa of the ten studied species of *Pleurodema*. Information of the other species included in the taxon sampling of Faivovich et al. (2012) was taken from literature (see sources in Table 2) but, unfortunately, many taxa have extensive missing data. Multistate characters were treated as nonadditive. Optimization was performed using the software Winclada (Nixon, 2002), using the command Optimization/Unambig changes only. Terminology used for ultrastructural sperm descriptions follows Aguiar-Jr et al. (2006) and anuran taxonomy follows Frost (2015). This study was carried out according to the regulations specified by the Institutional Animal Care and Use Committee of the Facultad de Ciencias Exactas y Naturales, UBA (Res C/D 140/00). The collection of *Pleurodema diplolister* was authorized by the Brazilian Institute for the Environment and Renewable Natural Resources (IBAMA – process 02001.002/2005/16).

## RESULTS

Ultrastructurally, the spermatozoa of the ten studied species of *Pleurodema* are elongate and filiform, consisting of three conspicuous regions: head (acrosome complex and nucleus), midpiece, and tail. Detailed descriptions of the ultrastructural morphology of spermatozoa are listed following similarities between species. Some structures, particularly membranes, were broken down in samples that had been fixed in formalin and stored in ethanol for extended periods of time. The main results are summarized in Table 1 and

general reconstructions of sperm morphology in Figures 8 and 9.

### *Pleurodema brachyops*, *P. cordobae*, and *P. kriegi* (Figs. 1 and 8A)

The acrosome complex is located at the anterior portion of the head, symmetrically covering the anterior part of the nucleus. It consists of two conical structures, the acrosome vesicle and a subacrosomal cone below. The acrosome vesicle extends from the tip of the cell to the anterior region of the nucleus, ending basally with a bulb-shaped thickening, whereas the subacrosomal cone extends beyond the base of the acrosome (Fig. 1A). The acrosome vesicle is membrane-bound and filled with homogeneous material of moderate electron density. In cross-section, the acrosome vesicle is circular and thicker in its medial region. The subacrosomal cone is formed by bundles of electron-dense material, not bound by a membrane and oriented approximately parallel to the longitudinal axis of the cell. This structure is continuous in longitudinal sections but discontinuous in transverse sections (Fig. 1B,C). The subacrosomal cone is separated from the nucleus by a reduced subacrosomal space (Fig. 1A). The nucleus is conical in longitudinal section and circular in transverse section (Fig. 1A,C–E). The chromatin is not fully compacted, and electron-lucent nuclear lacunae are occasionally observed in the anterior portion (Fig. 1C). The apical region, the nuclear rostrum, is narrow and protrudes into the acrosome complex. Posteriorly, the nucleus is surrounded by cytoplasm containing mitochondria and numerous cytoplasmic vacuoles (Fig. 1D–F).

The midpiece connects the head to the tail and consists of two centrioles, proximal and distal, which are surrounded by electron-dense material, the pericentriolar material. The proximal centriole lies in the nuclear fossa, whereas the distal centriole is perpendicular to the proximal and located outside the nuclear fossa (Fig. 1F). The posterior region of the midpiece consists of cytoplasm with ovoid and round mitochondria; this cytoplasm extends along the anterior portion of the tail, surrounding the flagellum (Fig. 1F,G).

The anterior region of the tail consists of an axoneme (with the typical $9 + 2$ pattern of microtubules) and a paraxonemal rod (Fig. 1G). In the middle region, the paraxonemal rod is modified in a juxtaxonemal fiber and an undulating membrane, which accompanies the axoneme (Fig. 1H). The terminal region of the tail contains only the axoneme (Fig. 1I).

### *Pleurodema diplolister* (Figs. 2A–D and 8B)

The acrosome complex is similar to the species described above. The nucleus has highly condensed chromatin (Fig. 2A,D–F). Posteriorly to the nucleus there is a nuclear fossa and two centrioles with the typical arrangement, surrounded by pericentriolar material (Fig. 2F,G). There are mitochondria in the midpiece and posteriorly they are arranged inside a mitochondrial collar (Fig. 2F–I).

The anterior portion of the tail consists only of the axoneme and paraxonemal rod, while in the middle region a juxtaxonemal fiber adjacent to the axoneme with an undulating membrane is observed (Fig. 2I–K). Only the axoneme extends until the terminal region of the tail (Fig. 2L).

### *Pleurodema marmoratum* (Figs. 3 and 8C)

The thin symmetric acrosome vesicle surrounds only the anteriormost portion of the nucleus. The subacrosomal cone lies below the acrosome vesicle; it extends over the nucleus, beyond the posterior end of the acrosome (Fig. 3A). In transverse section, the subacrosomal cone appears as a continuous ring composed of thick and dense homogeneous material (Fig. 3B–D). The subacrosomal cone is separated from the nucleus by a pronounced subacrosomal space. The anterior tip of the nucleus has the shape of a truncated cone, whereas the posterior end is surrounded by a cytoplasm with mitochondria (Fig. 3A,E,F). The nuclear fossa is conspicuous (Fig. 3G). The chromatin is highly condensed and electron-dense (Fig. 3A,C–F).

In the midpiece, both centrioles are embedded in pericentriolar material. Mitochondria are arranged inside a mitochondrial collar that surrounds the anterior region of the tail (Fig. 3G,H). In this region, the axoneme is associated with a paraxonemal rod, both of which are separated from the mitochondrial collar by the cytoplasmic canal (Fig. 3H). The mitochondrial collar and the paraxonemal rod distally disappear and the axoneme is linked to the undulating membrane through the juxtaxonemal fiber (Fig. 3I,J). The end of the spermatozoon tail is formed only by an axoneme (Fig. 3K).

### *Pleurodema guayapae* (Fig. 4)

The acrosome complex consists of a short and symmetrical acrosome and a subacrosomal cone, which ends at the anteriormost portion of the nucleus (Fig. 4A). In cross section, the subacrosomal cone is a continuous ring comprising dense homogeneous material (Fig. 4B–D). The apical region of the nucleus is conical and is separated from the acrosome complex by a reduced subacrosomal space. The acrosome vesicle is thick and the bulb-shaped ending is not observed. The nucleus has moderately condensed chromatin (Fig. 4A,D–F).

In the midpiece there are transverse striations around the centrioles (Fig. 4G). There is a mitochondrial collar in the posterior portion of the midpiece (Fig. 4H,I). Tail morphology is similar to that observed in the species described above (Fig. 4J).

*TABLE 1. Ultrastructural characteristics of the spermatozoa of Pleurodema species*

| | Head | | | | Midpiece | | Tail | | |
|---|---|---|---|---|---|---|---|---|---|
| | Acrosomal complex | | | | | | | | |
| | Acrosome vesicle | Subacrosomal cone | Subacrosomal space | Nucleus | Anterior region | Posterior region | Anterior region | Middle region | Terminal region |
| *P. brachyops*<br>*P. cordobae*<br>*P. kriegi* | Thick (T)<br>Short (L) | Discontinuos (T)<br>Medium (L) | Reduced | -Moderately condensed chromatin<br>-Nuclear lacunae | -Perpendicular centrioles<br>-Moderate pericentriolar material | -Cytoplasm around the flagellum | -Axoneme<br>-Paraxonemal rod | -Axoneme<br>-Juxtaxonemal fiber<br>-Undulating membrane | -Axoneme |
| *P. diplolister* | Thick (T)<br>Short (L) | Discontinuos (T)<br>Medium (L) | Pronounced | -Highly condensed chromatin | -Perpendicular centrioles<br>-Moderate pericentriolar material | -Mitochondrial collar around the flagellum | -Axoneme<br>-Paraxonemal rod | -Axoneme<br>-Juxtaxonemal fiber<br>-Undulating membrane | -Axoneme |
| *P. marmoratum* | Thin (T)<br>Short (L) | Continuos (T)<br>Extensive (L) | Pronounced | -Highly condensed chromatin | -Perpendicular centrioles<br>-Moderate pericentriolar material | -Mitochondrial collar around the flagellum | -Axoneme<br>-Paraxonemal rod | -Axoneme<br>-Juxtaxonemal fiber<br>-Undulating membrane | -Axoneme |
| *P. guayapae* | Thick (T)<br>Short (L) | Continuos (T)<br>Short (L) | Reduced | -Moderately condensed chromatin | -Perpendicular centrioles<br>-Transverse striations | -Mitochondrial collar around the flagellum | -Axoneme<br>-Paraxonemal rod | -Axoneme<br>-Juxtaxonemal fiber<br>-Undulating membrane | -Axoneme |
| *P. bufoninum* | Thick (T)<br>Extensive (L) | Reduced (T)<br>Extensive (L) | Absent | -Highly condensed chromatin | -Perpendicular centrioles<br>-Moderate pericentriolar material | -Mitochondrial collar around the flagellum | -Axoneme<br>-Paraxonemal rod | -Axoneme<br>-Paraxonemal rod | -Axoneme |
| *P. tucumanum* | Thick (T)<br>Short (L) | Discontinuos (T)<br>Short (L) | Pronounced | -Moderately condensed chromatin | -Perpendicular centrioles<br>-Scarce pericentriolar material | -Cytoplasm around the flagellum | -Axoneme | -Axoneme | -Axoneme |
| *P. borellii*<br>*P. cinereum* | Thin (T)<br>Short (L) | Discontinuos (T)<br>Medium (L) | Pronounced | -Moderately condensed chromatin<br>-Nuclear lacunae | -Perpendicular centrioles<br>-Moderate pericentriolar material | -Mitochondrial collar around the flagellum | -Axoneme<br>-Cytoplasmic sheath | -Axoneme<br>-Cytoplasmic sheath | -Axoneme |
| *P. thaul* | Thick (T)<br>Short (L) | Absent | Reduced | -Moderately condensed chromatin | -Perpendicular centrioles | -Cytoplasm around the flagellum | -Axoneme<br>-Paraxonemal rod<br>-Abaxonemal bulb-shaped swelling | -Axoneme<br>-Paraxonemal rod<br>-Abaxonemal bulb-shaped swelling | -Axoneme |

Data of *Pleurodema thaul* obtained from Pugin and Garrido (1981).
L, longitudinal section; T, transversal section.

*TABLE 2. Data matrix of ultrastructural characters of spermatozoa*

| Taxon | Characters | | | | | | | | | Reference |
|---|---|---|---|---|---|---|---|---|---|---|
| | 0 | 1 | 2 | 3 | 4 | 5 | 6 | 7 | 8 | |
| Leptodactylidae | | | | | | | | | | |
| Leiuperinae | | | | | | | | | | |
| *Pleurodema alium* | ? | ? | ? | ? | ? | ? | ? | ? | ? | |
| *Pleurodema bibroni* | ? | ? | ? | ? | ? | ? | ? | ? | ? | |
| *Pleurodema borellii* | 2 | 0 | 1 | 1 | 0 | 0 | – | – | 0 | *a* |
| *Pleurodema brachyops* | 2 | 0 | 0 | 0 | 1 | 0 | – | – | 1 | *a* |
| *Pleurodema bufoninum* | 1 | 0 | 1 | 0 | 1 | 1 | 1 | 0 | 0 | *a* |
| *Pleurodema cinereum* | 2 | 0 | 1 | 1 | 0 | 0 | – | – | 0 | *a* |
| *Pleurodema cordobae* | 2 | 0 | 0 | 0 | 1 | 0 | – | – | 1 | *a* |
| *Pleurodema diplolister* | 2 | 0 | 0 | 0 | 1 | 0 | – | – | 1 | *a* |
| *Pleurodema guayapae* | 2 | 0 | 0 | 0 | 1 | 0 | – | – | 1 | *a* |
| *Pleurodema kriegi* | 2 | 0 | 0 | 0 | 1 | 0 | – | – | 1 | *a* |
| *Pleurodema marmoratum* | 2 | 0 | 0 | 0 | 1 | 0 | – | – | 1 | *a* |
| *Pleurodema nebulosum* | ? | ? | ? | ? | ? | ? | ? | ? | ? | |
| *Pleurodema thaul* | 0 | 0 | 0 | 0 | 1 | 1 | 1 | 1 | 0 | *b* |
| *Pleurodema tucumanum* | 2 | 0 | 0 | 0 | 0 | 0 | – | – | 0 | *a* |
| *Pleurodema somuncurense* | ? | ? | ? | ? | ? | ? | ? | ? | ? | |
| *Physalaemus riograndensis* | ? | ? | ? | ? | ? | ? | ? | ? | ? | |
| *Physalaemus biligonigerus* | 2 | 1 | 1 | 0 | 1 | 0 | – | – | 1 | *c* |
| *Physalaemus barrioi* | ? | ? | ? | ? | ? | ? | ? | ? | ? | |
| *Physalaemus cuvieri* | ? | ? | ? | ? | ? | ? | ? | ? | ? | |
| *Physalaemus signifier* | ? | ? | ? | ? | ? | ? | ? | ? | ? | |
| *Physalaemus nattereri* | 2 | 1 | 1 | 0 | 1 | 0 | – | – | 1 | *d* |
| *Physalaemus santafecinus* | ? | ? | ? | ? | ? | ? | ? | ? | ? | |
| *Engystomops guayaco* | ? | ? | ? | ? | ? | ? | ? | ? | ? | |
| *Engystomops pustulatus* | ? | ? | ? | ? | ? | ? | ? | ? | ? | |
| *Edalorhina perezi* | ? | ? | ? | ? | ? | ? | ? | ? | ? | |
| *Pseudopaludicola falcipes* | 2 | 1 | 1 | 0 | 1 | 1 | 0 | 0 | 1 | *e* |
| Leptodactylinae | | | | | | | | | | |
| *Leptodactylus latrans* | 0 | 0 | 0 | 0 | 1 | 1 | 0 | 0 | 1 | *f* |
| *Lithodytes lineatus* | 0 | 0 | 0 | 0 | 1 | 1 | 0 | 0 | 1 | *f* |
| Paratelmatobiinae | | | | | | | | | | |
| *Paratelmatobius* sp. | ? | ? | ? | ? | ? | ? | ? | ? | ? | |
| Allophrynidae | | | | | | | | | | |
| *Allophryne ruthveni* | ? | ? | ? | ? | ? | ? | ? | ? | ? | |
| Aromobatidae | | | | | | | | | | |
| *Allobates femoralis* | 2 | 0 | 1 | 0 | 0 | 1 | – | 0 | 1 | *g* |
| Batrachylidae | | | | | | | | | | |
| *Batrachyla leptopus* | 2 | 1 | 1 | 0 | 1 | 1 | – | 0 | 1 | *b, h* |
| Bufonidae | | | | | | | | | | |
| *Melanoprhyniscus klappenbachi* | ? | ? | ? | ? | ? | ? | ? | ? | ? | |
| Centrolenidae | | | | | | | | | | |
| *Espadarana prosoblepon* | ? | ? | ? | ? | ? | ? | ? | ? | ? | |
| Ceratophryidae | | | | | | | | | | |
| *Ceratophrys cranwelli* | 2 | 0 | 1 | 0 | 1 | 1 | 0 | 0 | 1 | *i* |
| Cycloramphidae | | | | | | | | | | |
| *Cycloramphus boraceiensis* | ? | ? | ? | ? | ? | ? | ? | ? | ? | |
| Odontophrynidae | | | | | | | | | | |
| *Odontophrynus americanus* | ? | ? | ? | ? | ? | ? | ? | ? | ? | |
| Hylidae | | | | | | | | | | |
| *Litoria caerulea* | 2 | 0 | 1 | 0 | 1 | 1 | 0 | 0 | 1 | *i, j* |
| Hylodidae | | | | | | | | | | |
| *Crossodactylus schmidti* | ? | ? | ? | ? | ? | ? | ? | ? | ? | |
| Telmatobiidae | | | | | | | | | | |
| *Telmatobius bolivianus* | ? | ? | ? | ? | ? | ? | ? | ? | ? | |

Character-states were scored on the taxon sampling employed by Faivovich et al. (2012). See text for further information. Missing data are indicated by a question mark and inapplicable data by a dash.

[a]Present study.
[b]Pugin and Garrido (1981).
[c]Amaral et al. (1999).
[d]Zieri et al. (2008).
[e]Amaral et al. (2000).
[f]Salles et al. (2015).
[g]Aguiar-Jr et al. (2003).
[h]Garrido et al. (1989).
[i]Scheltinga (2002).
[j]Lee and Jamieson (1993).

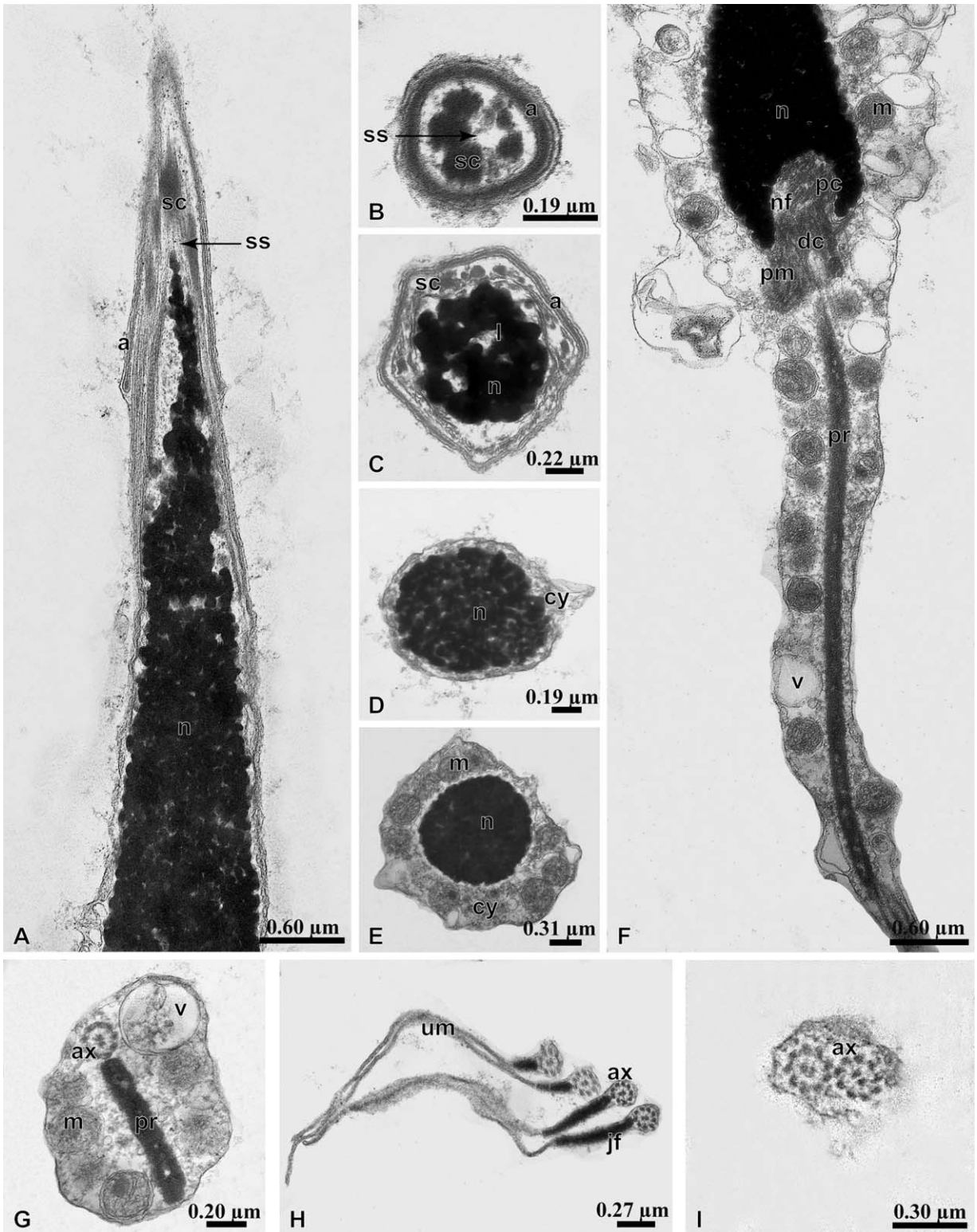


Fig. 1. Transmission electron micrographs of spermatozoa *of Pleurodema brachyops*, *P. cordobae*, and *P. kriegi*. **A**: Longitudinal section (LS) of the acrosome complex and nucleus showing the acrosomal vesicle and subacrosomal cone. **B**: Transverse section (TS) through the acrosome complex showing a thick acrosome vesicle and the convergent bundles of fibers belonging to the subacrosomal cone. **C**: TS of the acrosome complex-nucleus showing the acrosomal vesicle, the subacrosomal cone and the nucleus with chromatin with electron-lucent nuclear lacunae. **D–E**: TSs through the nucleus. Note the mitochondria in the cytoplasm surrounding the posterior region of the nucleus. **F**: LS of posterior region of the nucleus, midpiece, and tail. Note in the midpiece the arrangement of the centrioles surrounded by the pericentriolar material. **G**: TS of the anterior region of the tail showing cytoplasm with mitochondria and vacuoles surrounding the axoneme and the paraxonemal rod. **H**: TS of middle region of the tail showing the axoneme and the juxtaxonemal fiber continuous with the undulating membrane. **I**: TS of the terminal region of the tail where only the axoneme is observable. *Abbreviations*: a, acrosome vesicle; ax, axoneme; cy, cytoplasm; dc, distal centriole; jf, juxtaxonemal fiber; l, nuclear lacunae; m, mitochondria; n, nucleus; nf, nuclear fossa; pc, proximal centriole; pm, pericentriolar material; pr, paraxonemal rod; sc, subacrosomal cone; ss, subacrosomal space; um, undulating membrane; v, cytoplasmic vacuole.

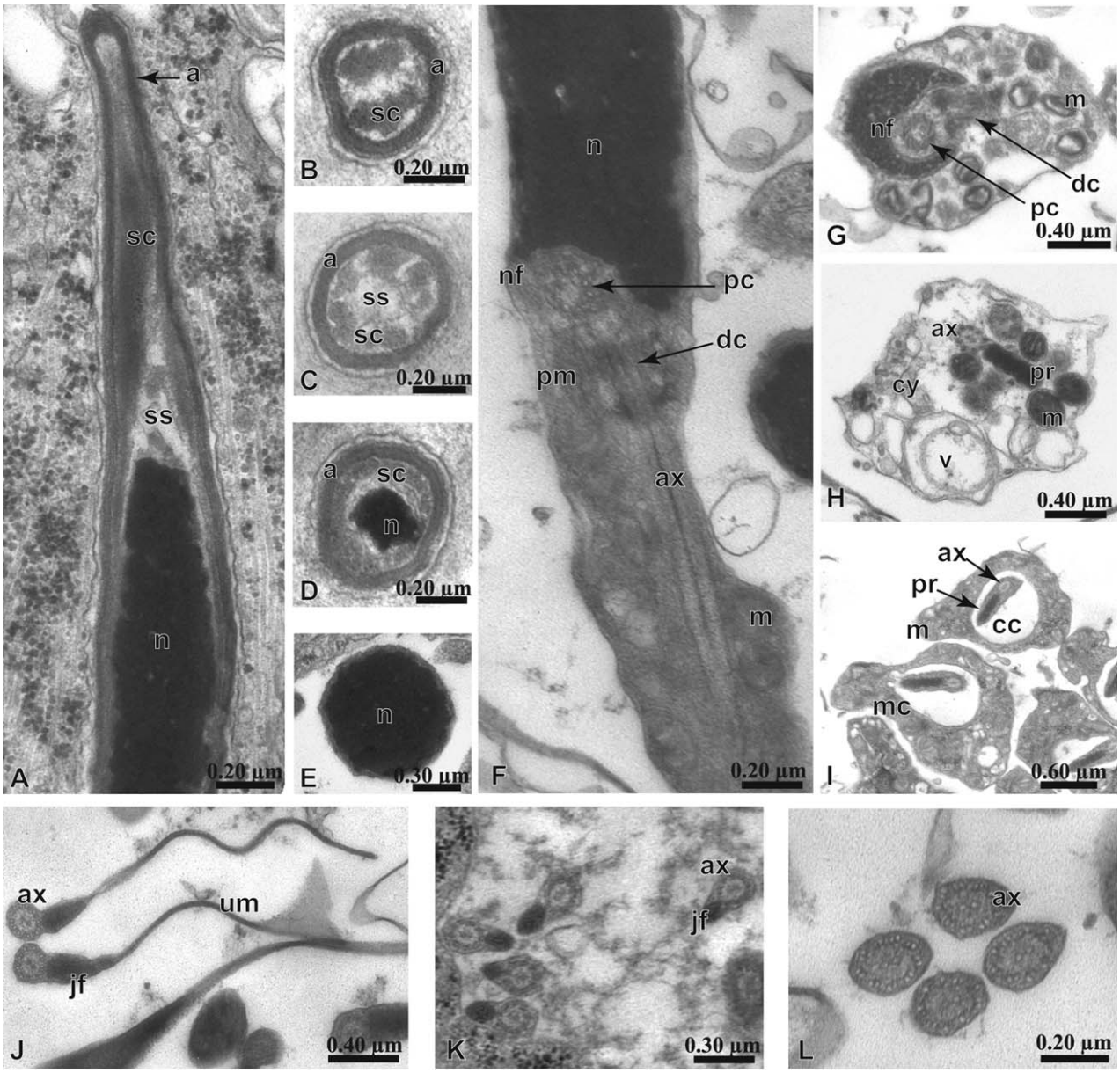


Fig. 2. Transmission electron micrographs of spermatozoa *of Pleurodema diplolister*. **A**: Longitudinal section (LS) of the acrosome complex and nucleus showing the acrosomal vesicle and subacrosomal cone. **B–E**: Transverse sections (TS) through the acrosome complex and nucleus showing a thick acrosome vesicle and the convergent bundles of fibers belonging to the subacrosomal cone. **F**: LS of posterior region of the nucleus, midpiece, and tail. Note in the midpiece the arrangement of the centrioles surrounded by the pericentriolar material and the disposition of the mitochondria around of the axoneme. **G–I**: TSs of midpiece and tail showing cytoplasm with mitochondria and vacuoles surrounding the axoneme and the paraxonemal rod. Note the presence of the mitochondrial collar in the most posterior region of the midpiece. **J–K**: TSs of middle region of the tail showing the axoneme and the justaxonemal fiber continuous with the undulating membrane. The undulating membrane decreases posteriorly. **L**: TS of the terminal region of the tail where only the axoneme is observable. *Abbreviations*: a, acrosome vesicle; ax, axoneme; cc, cytoplasmic canal; cy, cytoplasm; dc, distal centriole; jf, juxtaxonemal fiber; m, mitochondria; mc, mitochondrial collar; n, nucleus; nf, nuclear fossa; pc, proximal centriole; pm, pericentriolar material; pr, paraxonemal rod; sc, subacrosomal cone; ss, subacrosomal space; um, undulating membrane; v, cytoplasmic vacuole.

### *Pleurodema bufoninum* (Figs. 5 and 8D)

The acrosome complex is composed of an elongated and conical acrosome vesicle and an underlying reduced subacrosomal cone (Fig. 5A). The acrosome is thick and is filled with an electron-dense material. It extends posteriorly and ends with a bulb-shaped thickening (Fig. 5E). The subacrosomal cone is thin, extends beyond the acrosome vesicle and is filled with a less electron-dense material than in the acrosome (Fig. 5A–E); it is in close contact with the nucleus so that no subacrosomal space can be observed (Fig. 5A,E).

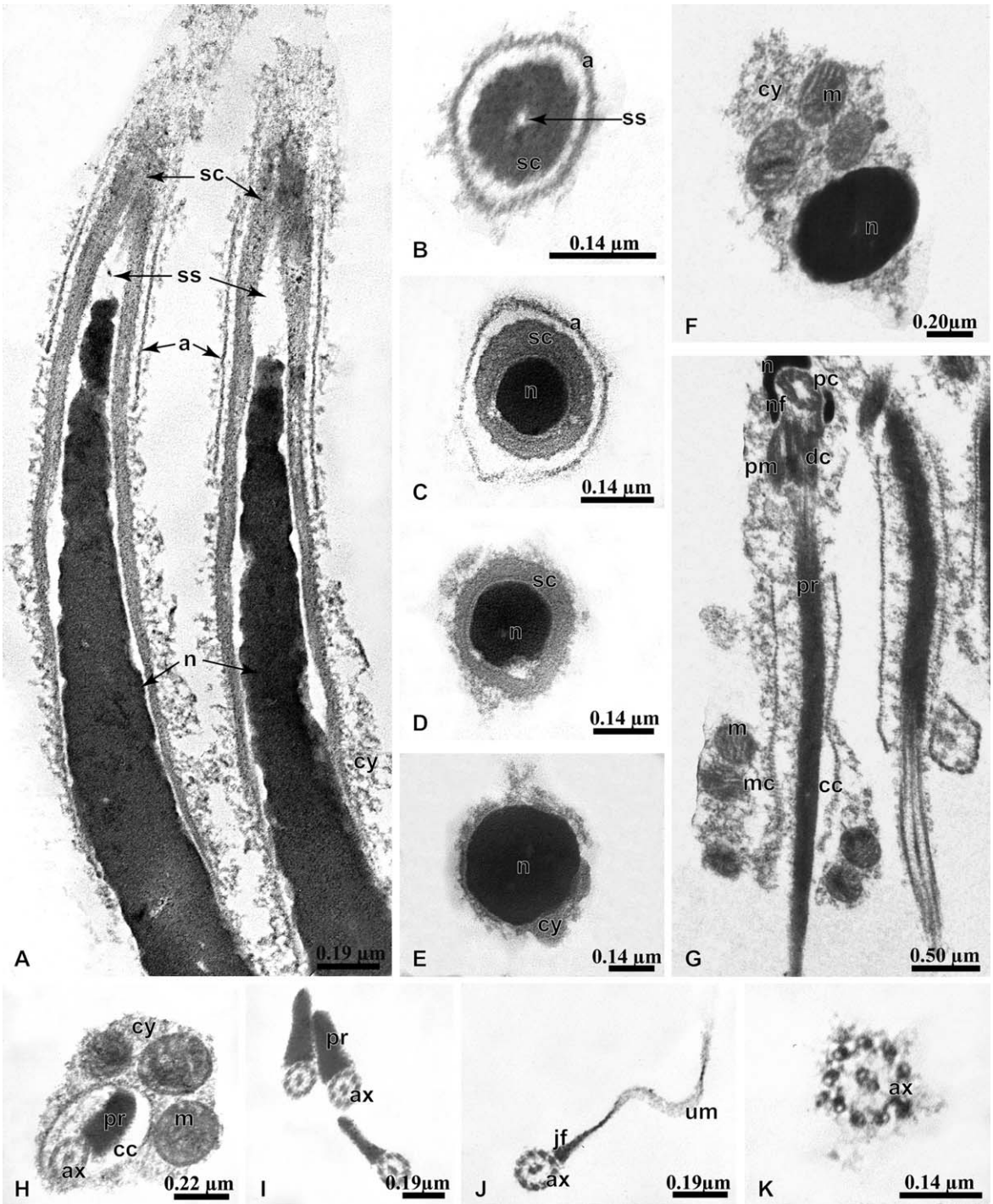


Fig. 3. Transmission electron micrographs of spermatozoa of *Pleurodema marmoratum*. **A**: Longitudinal section (LS) of the acrosome complex and nucleus. Note the great extension of the subacrosomal cone in relation to the acrosomal vesicle. **B**: Transverse section (TS) through the acrosome complex showing the acrosome vesicle and wide subacrosomal cone with the subacrosomal space. **C–E**: TSs at level of the nucleus. Note the subsequent disappearance of the acrosome vesicle and subacrosomal cone. **F**: TS of the posteriormost region of the nucleus surrounded by cytoplasm with mitochondria. **G**: LS of the midpiece and tail showing the nuclear fossa and the arrangement of centrioles. Note the mitochondrial collar surrounding the anterior portion of the tail separated by a cytoplasmic canal. **H**: TS of the mitochondrial collar of the midpiece. Note the axoneme and the paraxonemal rod. **I**: TS of the anterior region of the tail showing an axoneme and paraxonemal rod. **J**: TS of the middle region of the tail showing the axonema, juxtaxonemal fiber and the undulating membrane. **K**: TS of the terminal region of the tail where only the axoneme is observable. *Abbreviations*: a, acrosome vesicle; ax, axoneme; cc, cytoplasmic canal; cy, cytoplasm; dc, distal centriole; jf, juxtaxonemal fiber; m, mitochondria; mc, mitochondrial collar; n, nucleus; nf, nuclear fossa; pc, proximal centriole; pm, pericentriolar material; pr, paraxonemal rod; sc, subacrosomal cone; ss, subacrosomal space; um, undulating membrane.

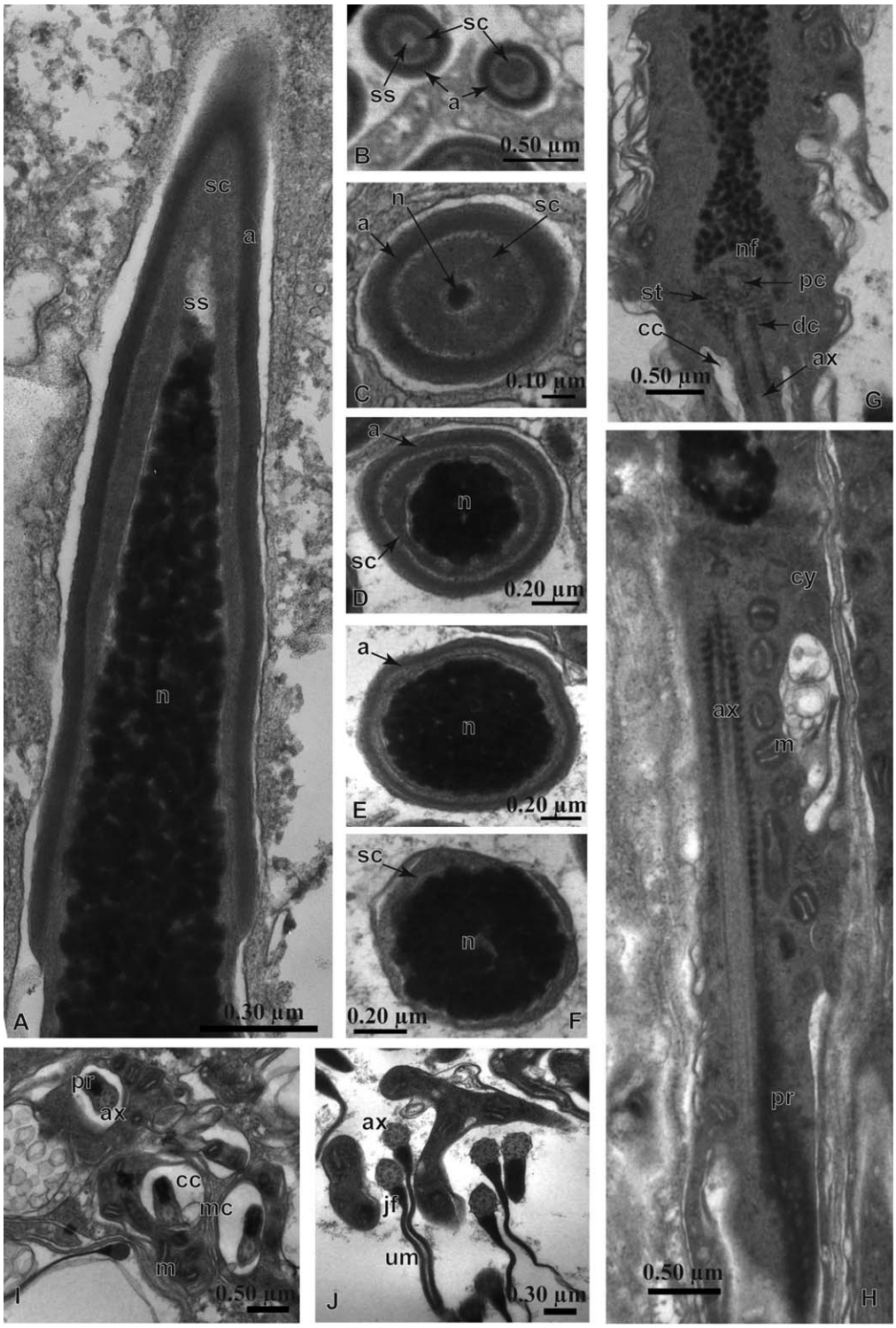


Fig. 4. Transmission electron micrographs of spermatozoa of *Pleurodema guayapae*. **A**: Longitudinal section (LS) of the acrosome complex and nucleus. **B**: Transverse section (TS) through the acrosome complex showing the width acrosome vesicle and subacrosomal cone. **C-F**: TSs at level of the nucleus. Note the subsequent disappearance of the acrosome vesicle and subacrosomal cone. **G**: LS of the midpiece and tail showing the nuclear fossa and the arrangement of centrioles. Note the presence of transverse striation surrounding proximal and distal centrioles. **H**: LS of the anterior region of the tail showing an axoneme and paraxonemal rod. **I**: TS of the mitochondrial collar of the midpiece. **J**: TS of the middle region of the tail showing the axoneme, juxtaxonemal fiber and the undulating membrane. *Abbreviations*: a, acrosome vesicle; ax, axoneme; cc, cytoplasmic canal; cy, cytoplasm; dc, distal centriole; jf, juxtaxonemal fiber; m, mitochondria; mc, mitochondrial collar; n, nucleus; nf, nuclear fossa; pc, proximal centriole; pr, paraxonemal rod; sc, subacrosomal cone; ss, subacrosomal space; st, transverse striation; um, undulating membrane.

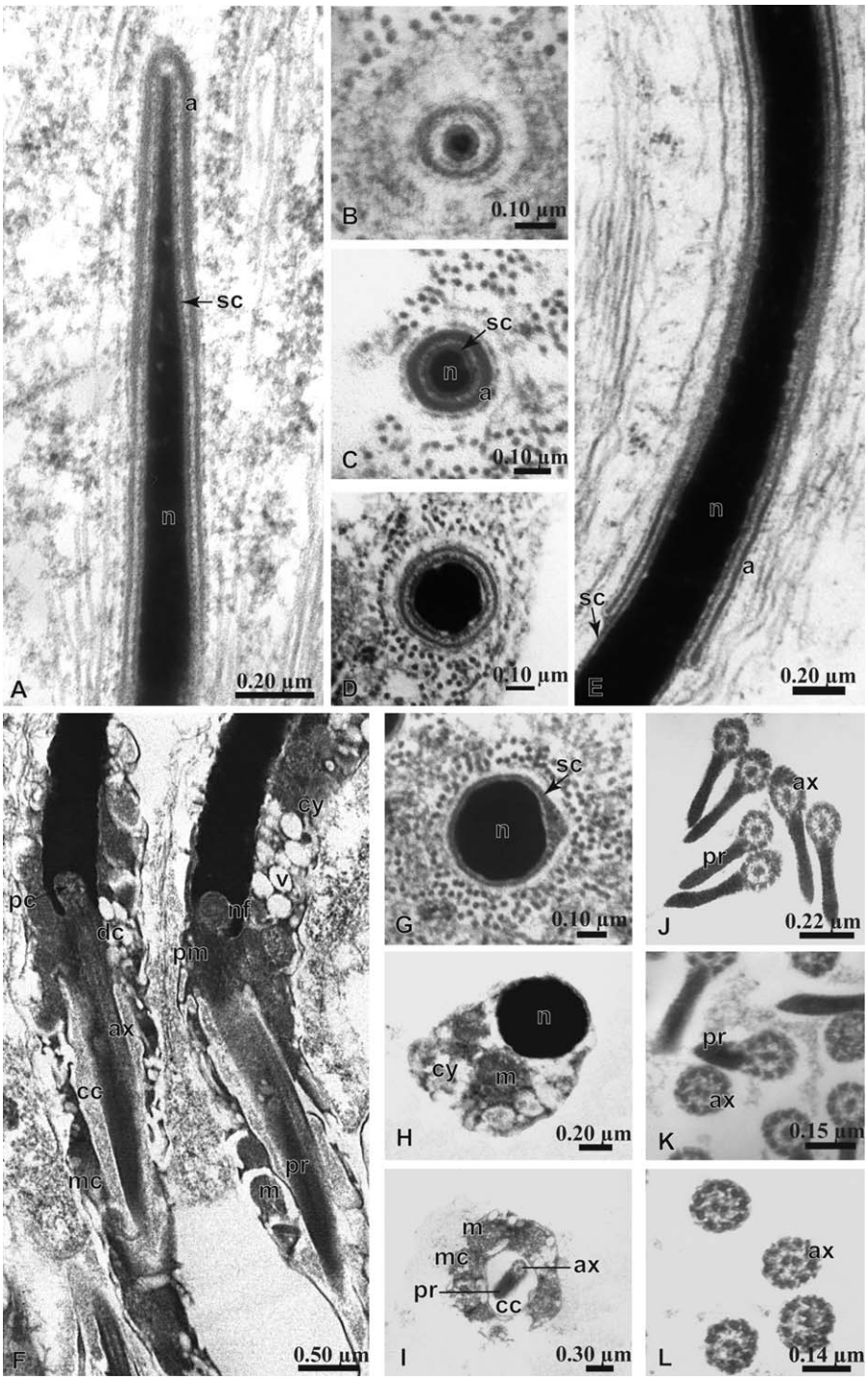


Fig. 5. Transmission electron micrographs of spermatozoa of *Pleurodema bufoninum*. **A**: Longitudinal section (LS) of the anterior region of the nucleus showing the acrosome vesicle and the subacrosomal cone. **B–D**: Transverse sections (TS) of the anterior region of the nucleus showing the acrosome vesicle and the subacrosomal cone. Note the close contact of the subacrosomal cone with the nucleus. **E**: LS of the middle region of the nucleus. Note the extension of the acrosome vesicle and the subacrosomal cone towards the posterior region of the nucleus. **F**: LS of the terminal region of the nucleus, midpiece, and anterior region of the tail showing the nuclear fossa and the arrangement of the centrioles, continued by the tail surrounded by a mitochondrial collar and separated from this by a cytoplasmic canal. **G**: TS at middle level of the nucleus showing the subacrosomal cone. **H**: TS at level of the posterior region the nucleus surrounded by cytoplasm containing mitochondria. **I–L**: TS of the tail. Note the presence of a mitochondrial collar and only paraxonemal rod accompanying the axoneme in the anterior region of the tail. *Abbreviations*: a, acrosome vesicle; ax, axoneme; cc, cytoplasmic canal; cy, cytoplasm; dc, distal centriole; m, mitochondria; mc, mitochondrial collar; n, nucleus; nf, nuclear fossa; pc, proximal centriole; pm, pericentriolar material; pr, paraxonemal rod; sc, subacrosomal cone; v, cytoplasmic vacuole.

The cylindro-conical nucleus tapers to a rounded tip within the acrosome complex. The chromatin is highly condensed and electron-dense (Fig. 5A–H). The posteriormost portion of the nucleus is surrounded by cytoplasm with numerous vacuoles and mitochondria (Fig. 5F,H). The centrioles are surrounded by pericentriolar material. There is a mitochondrial collar in the posterior region of the midpiece (Fig. 5F,I). The anterior and middle regions of the tail are composed of an axoneme and a paraxonemal rod. A cytoplasmic canal separates this region from the mitochondrial collar (Fig. 5I–K). The posterior portion of the tail is formed only by the axoneme (Fig. 5L).

### *Pleurodema tucumanum* (Figs. 6 and 9A)

The spermatozoon head is blunt at its anterior tip. The acrosome complex, formed by short and symmetric acrosome and subacrosomal cone, ends at the anteriormost portion of the nucleus (Fig. 6A). The thick acrosome contains moderately electron-dense material and ends basally with a bulb-shaped thickening (Fig. 6A–E). The subacrosomal cone is discontinuous in transverse section, and it consists of longitudinal bundles of electron-dense material (Fig. 6B–D). The acrosome complex is separated from the apical tip of the nucleus by a pronounced subacrosomal space (Fig. 6A).

The nucleus has a rounded apical tip, it is conical in longitudinal section and circular in cross section, and is composed of moderately condensed chromatin (Fig. 6A,D–H). The posterior region of the nucleus is surrounded by cytoplasm with few mitochondria (Fig. 6F).

In the midpiece, the proximal centriole lies within the symmetrical nuclear fossa. The proximal centriole is surrounded by dense and scarce pericentriolar material that connects it with the nuclear fossa and with the distal centriole (Fig. 6G,H). The cytoplasm of the anterior portion of the axoneme contains several mitochondria and vacuoles (Fig. 6G–I). The mitochondrial collar is absent.

The terminal region of the tail is composed only of an axoneme (Fig. 6J). Accessory fibers and undulating membrane are absent.

### *Pleurodema borellii* and *P. cinereum* (Figs. 7 and 9B)

The acrosome vesicle contains electron-lucent material, is thin and the bulb-shaped ending is not observed. The subacrosomal cone extends slightly beyond the vesicle (Fig. 7A); it appears as a moderately electron-dense structure discontinuous in transverse section, composed of coarse fibers forming irregular isolated bundles (Fig. 7B,C). The nucleus has granular moderately condensed chromatin, with some electron-lucent lacunae (Fig. 7A,C–E); it is surrounded by a sheath of cytoplasm containing mitochondria that increase in number toward the tail (Fig. 7E,F). Two centrioles are present within the centriolar region, with the proximal centriole being inside the nuclear fossa and the distal one being outside it; both centrioles are surrounded by moderate pericentriolar material. The posteriormost portion of the midpiece contains a mitochondrial collar separated from the tail by a cytoplasmic canal (Fig. 7F). The anterior region of the tail shows an axoneme surrounded by a sheath of cytoplasm, which exhibits different electron-densities (Fig. 7F–H). The amount of cytoplasm surrounding the axoneme decreases toward the end of the tail, where only the axoneme is observed (Fig. 7I).

## Character Definition

Nine characters were described according to the observed variability. Characters 3–8 were coded at the medial region of the tail (see sections F of Figs. 8 and 9). The data matrix is shown in Table 2. The optimization of the characters described below is discussed in the next section and illustrated in Figure 10.

0. *Subacrosomal cone*: (0) absent, (1) reduced, (2) developed. Figures 1A,C, 2A–D, 3A–D, 4A–D, 5A, C, E, 6A–E, and 7A–C.

   The subacrosomal cone is placed behind the acrosome vesicle and is formed by electron-dense material. Traditionally, this structure was named *subacrosomal cone* in *Ascaphus truei* (Jamieson et al., 1993) and *Leiopelma hochstetteri* (Scheltinga et al., 2001), and *conical perforatorium* in other anuran families where it occurs (e.g. Lee and Jamieson, 1992; see also Scheltinga, 2002). However, Garda et al. (2002) proposed the homology of the subacrosomal cone with the conical perforatorium. We agree with their arguments, as well as other recent papers (e.g., Aguiar-Jr et al., 2003, 2004, 2006; Garda et al. 2004; Zieri et al. 2008).

1. *Transverse striations at midpiece*: (0) absent, (1) present. Figure 4G.

   Cross striations can be observed in the midpiece, and seem to be continued with the paraxonemal rod (Reed and Stanley, 1972; Rastogi et al., 1988; Báo et al., 1991; Amaral et al., 2000).

2. *Mitochondrial collar* (*sensu* Lee and Jamieson, 1992): (0) absent, (1) present. Figures 2I, 3G, 4I, 5I, and 7F.

   The mitochondria can be distributed in a well-developed and cylindrical collar placed around the proximal region of the sperm tail (mitochondrial collar). When this structure is absent, the mitochondria are place along the tail, adjacent to the axoneme (Scheltinga, 2002).

3. *Cytoplasmatic sheath surrounding the axoneme*: (0) absent, (1) present. Figure 7F–H.

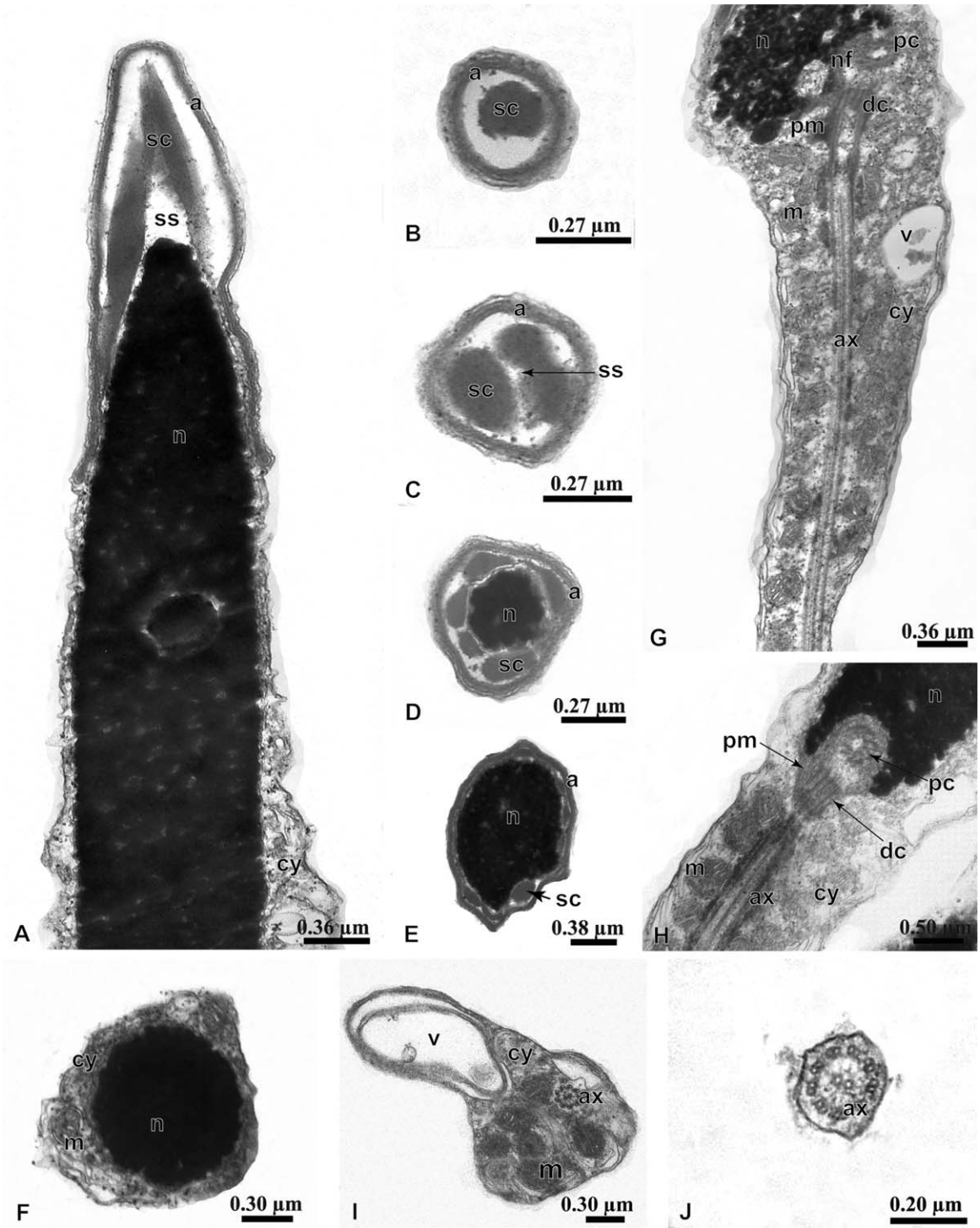


Fig. 6. Transmission electron micrographs of spermatozoa of *Pleurodema tucumanum*. **A**: Longitudinal section (LS) of the acrosome complex and nucleus showing the acrosome vesicle and the subacrosomal cone. **B–E**: Transverse sections (TS) of the acrosome complex and nucleus showing the discontinuous subacrosomal cone and the enlargement of the nucleus. **F**: TS of the posteriormost region of the nucleus surrounded by cytoplasm with mitochondria. **G**: LS of the terminal region of the nucleus, midpiece, and anterior region of the tail. **H**: LS of midpiece showing the nuclear fossa and the arrangement of the centrioles. **I**: TS of the anteriormost region of the tail showing cytoplasm with mitochondria surrounding the axoneme. Note the presence of a cytoplasmic vacuole. **J**: TS of the terminal region the tail showing the typical structure of the axoneme. *Abbreviations*: a, acrosome vesicle; ax, axoneme; cy, cytoplasm; dc, distal centriole; m, mitochondria; n, nucleus; nf, nuclear fossa; pc, proximal centriole; pm, pericentriolar material; sc, subacrosomal cone; ss, subacrosomal space; v, cytoplasmic vacuole.

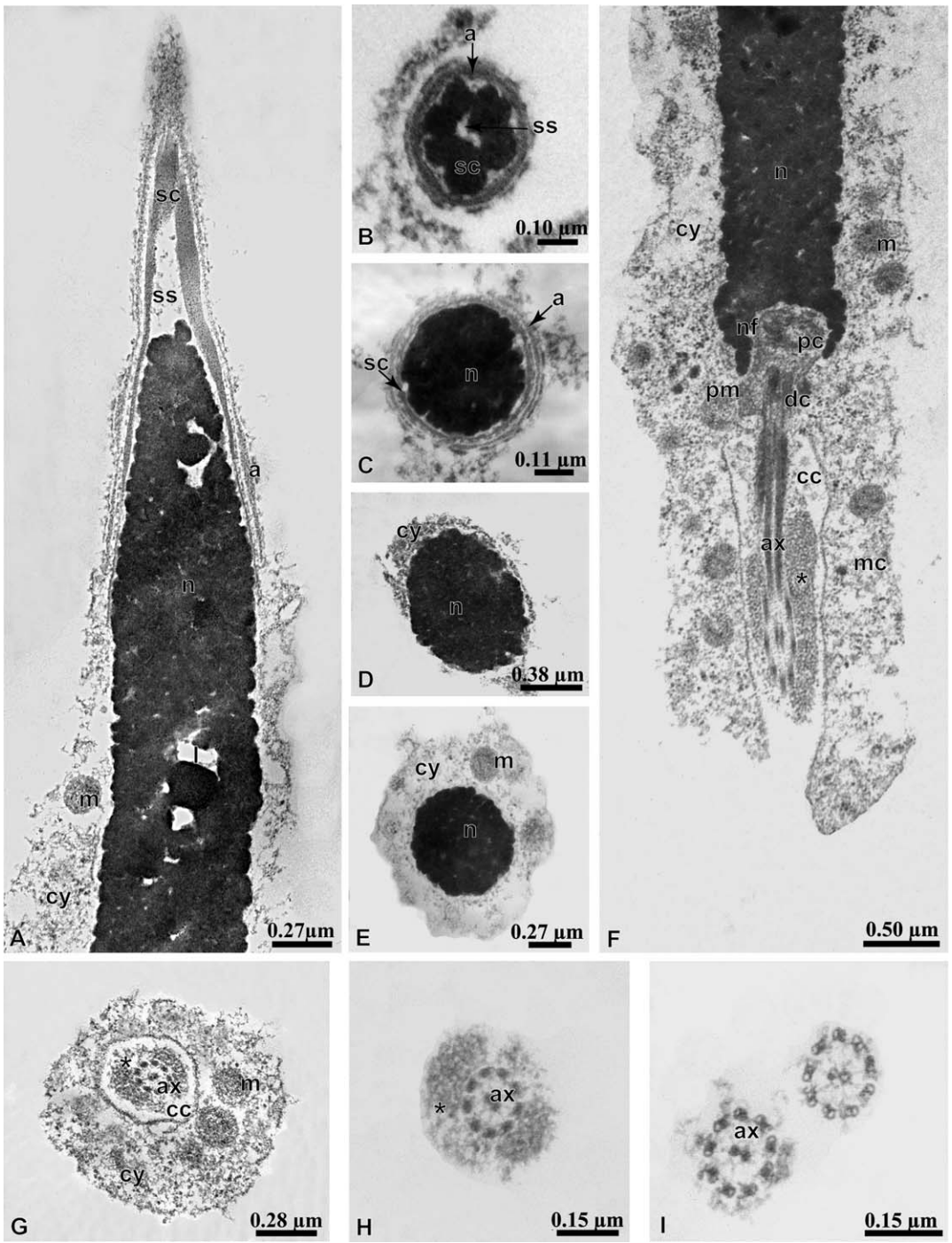


Fig. 7. Transmission electron micrographs of spermatozoa of *Pleurodema borellii* and *P. cinereum*. **A**: Longitudinal section (LS) of the acrosome complex and nucleus. **B**: Transverse section (TS) of the acrosome complex showing the discontinuous subacrosomal cone surrounded by the acrosome vesicle. **C**: TS at level of the acrosome complex-nucleus. **D**: TS of the anterior region of the nucleus surrounded by slight cytoplasm. **E**: TS of the posterior region of the nucleus. Note the presence of the mitochondria. **F**: LS at level of the nucleus, midpiece, and anterior region of the tail. Note the arrangement of the centrioles in relation to the nuclear fossa and the presence of a mitochondrial collar surrounding the tail, and a cytoplasmic sheath surrounding the axoneme (asterisk). **G**: Transverse section of the anterior region of the tail showing the axoneme surrounded by a mitochondrial collar separated by the cytoplasmic canal. Note a cytoplasmic sheath with areas of different electron-density surrounding the axoneme (asterisk) **H**: TS of the posterior region of the tail. Note the presence of a cytoplasmic sheath (asterisk). **I**: Terminal region of the tail formed only by the axoneme. *Abbreviations*: a, acrosome vesicle; ax, axoneme; cc, cytoplasmic canal; cy, cytoplasm; dc, distal centriole; l, nuclear lacunae; m, mitochondria; mc, mitochondrial collar; n, nucleus; nf, nuclear fossa; pc, proximal centriole; pm, pericentriolar material; sc, subacrosomal cone; ss, subacrosomal space.

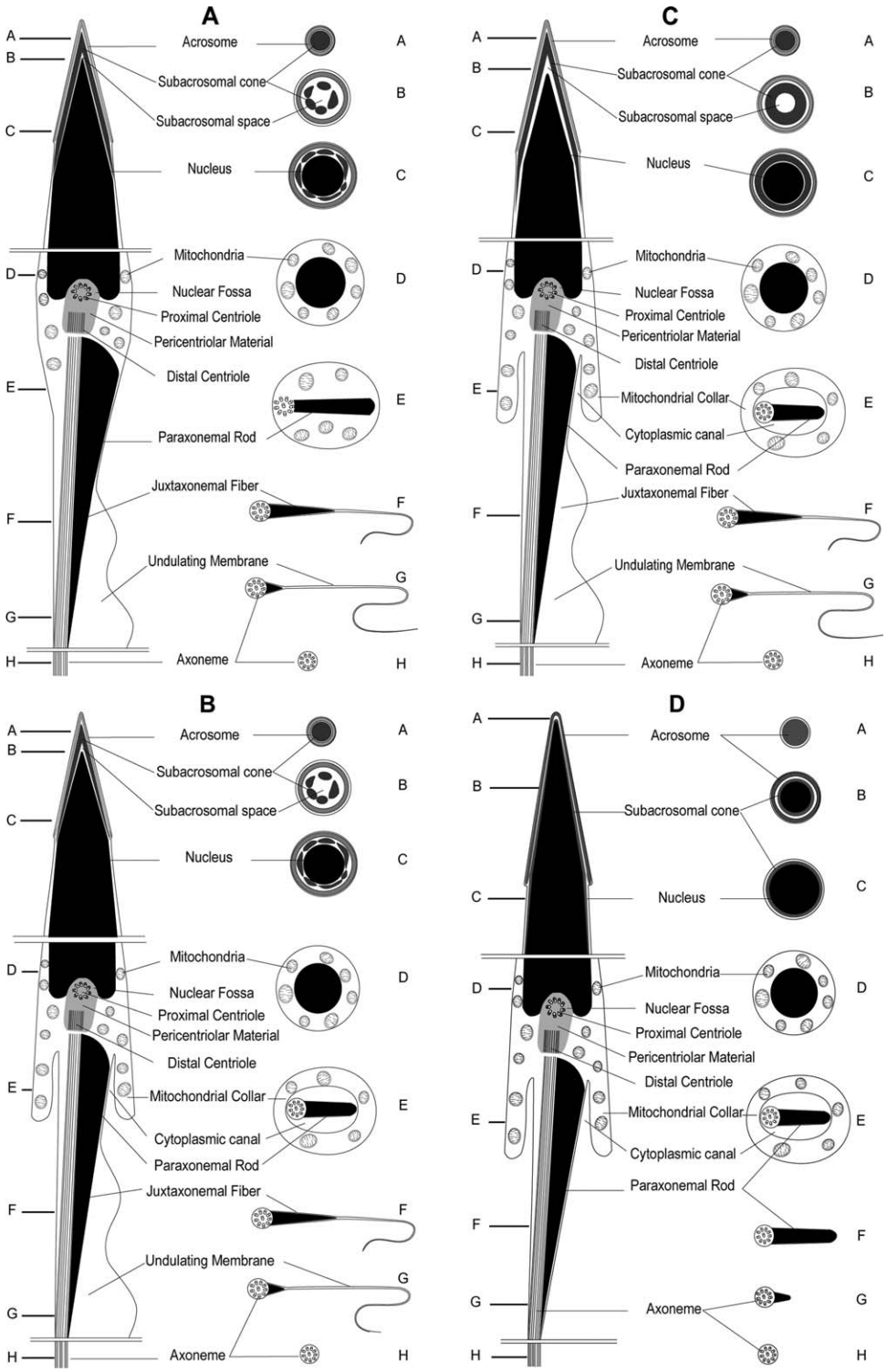


Fig. 8. Schematic reconstructions of the spermatozoa of **A**: *P. brachyops*, *P. cordobae*, and *P. kriegi*. **B**: *P. diplolister*. **C**: *P. marmoratum*. **D**: *P. bufoninum*.

A cytoplasmatic sheath surrounding the axoneme with different electron-densities has only been observed in *Pleurodema borellii* and *P. cinereum*.

4. *Juxtaxonemal fiber*: (0) absent, (1) present.
5. *Axial fiber*: (0) absent, (1) present.
6. *Paraxonemal rod*: (0) absent, (1) present. Figure 5J.

Characters 4–6 refer to the accessory fibers of the sperm tail. The generalized anuran sperm has two longitudinal fibers that accompany the axoneme: the juxtaxonemal fiber (= minor fibre *sensu* Lee

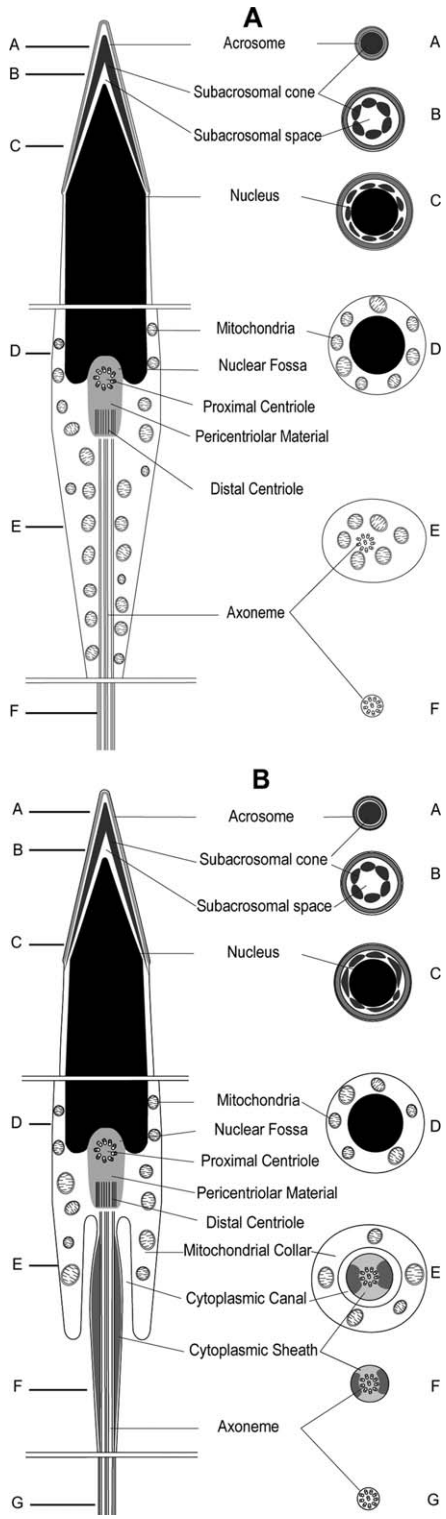


Fig. 9. Schematic reconstructions of the spermatozoa of **A**: *P. tucumanum*. **B**: *P. borellii* and *P. cinereum*.

and Jamieson, 1993) adjacent to doublet 3 of the axoneme, and the axial fiber (= major fibre *sensu* Lee and Jamieson, 1993 = axial rod *sensu* Amaral et al., 2000).

An axial fiber occurs in *Pseudopaludicola falcipes*, *P. mineira*, *P. saltica*, and *P. ternetzi* (Amaral et al., 2000; Santos et al., 2015). In these cases, the axial fiber is attached to the juxtaxonemal fiber by a thin cytoplasmic lamina, the undulating membrane (characters 4:1; 5: 1, 6: 0). The spermatozoa of all studied *Pleurodema* lack a discrete axial fiber.

In some cases, the axial and juxtaxonemal fibers are not distinguishable. According to Lee and Jamieson (1993: 310), in their definition of a "generalized pelodryadid-bufonid spermatozoon," they observed an electron-dense "paraxonemal rod," initially round in cross-section, which begins posterior to the distal centriole and runs beside the axoneme for a short distance. In these species, the paraxonemal rod gradually splits into unequal portions as a constriction, and then an undulating membrane, develops between its two portions (distinct axial and juxtaxonemal fibers).

Scheltinga (2002: 54) described, for the former *Cyclorana brevipes* group (now in the genus *Litoria*, Hylidae), that the axial and juxtaxonemal fibers are not distinguishable; and that a short and thick electron-dense rod occurs within the undulating membrane and is termed the paraxonemal rod. This last condition, developed throughout the tail, is what we observed in *Pleurodema bufoninum* (Fig. 5J) and *P. thaul* (Pugin and Garrido, 1981). Also, this condition has recently been reported for several species *Pseudopaludicola* (*Pseudopaludicola canga*, *P. giarettai*, *P. atragula*, *P. facureae*, and *P. mystacalis*; Santos et al. 2015).

7. *Occurrence of an abaxonemal bulb-shaped swelling*: (0) absent, (1) present.

   This structure also refers to the accessory fibers of the sperm tail. The paraxonemal rod can possess a distinct bulb at the abaxonemal end (character 7: 1). This feature was described for *Pleurodema thaul*, and it was interpreted as the axial fiber (Pugin and Garrido, 1981, their fig. 39).
8. *Undulating membrane*: (0) absent, (1) present, adaxonemal. Figures 1H, 2J, 3J, and 4J.

   A unilateral undulating membrane occurs in the mature spermatozoa of many anuran families, usually accompanied either by the juxtaxonemal fiber or by the axial fiber (Scheltinga and Jamieson, 2003). Although the undulating membrane commonly develops at the adaxonemal end of the juxtaxonemal fiber, in *Engystomops pustulosus* it extends from the abaxonemal end of the axial fiber (Scheltinga 2002, not included in the data matrix).

## DISCUSSION

The ultrastructure of the spermatozoa of the ten species of *Pleurodema* studied here shows an unusual mosaic of features. The characters

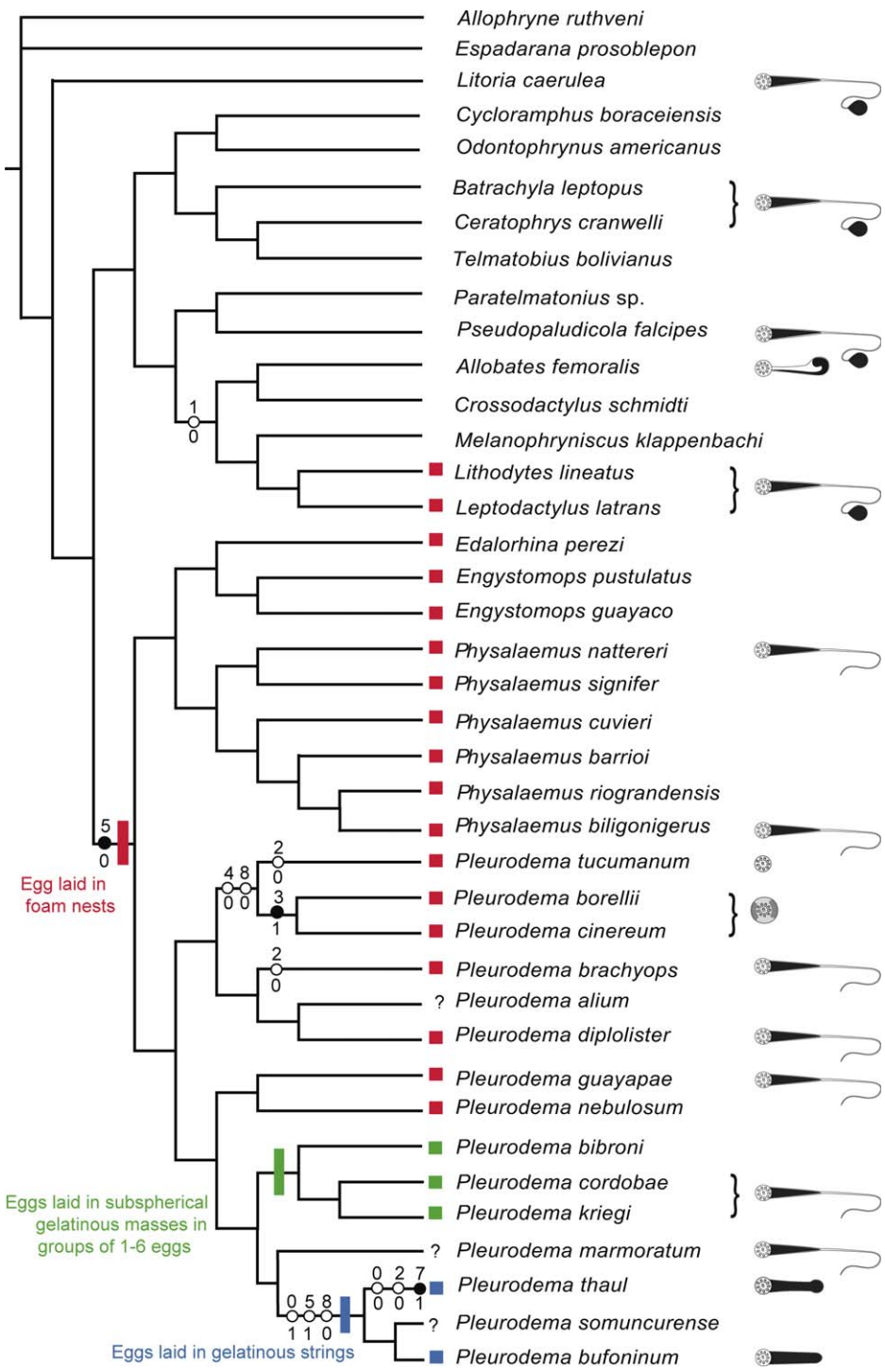


Fig. 10. Optimization of ultrastructural characters of the spermatozoa on the phylogenetic hypothesis of *Pleurodema* proposed by Faivovich et al. (2012), based on their Figure 6. See list of characters and literature sources in Table 2. *Black circles* indicate non-homoplastic transformations and *white circles* homoplastic transformations. Numbers above and below the circles indicate number and states of characters, respectively. Egg-clutch structure of leptodactylids species included is denoted with colored squares: eggs laid in foam nests (red squares), eggs laid in subspherical gelatinous masses in groups of 1–6 eggs (green squares), and eggs laid in gelatinous strings (blue squares). Schematic representations of tails (at middle region) are included for species for which spermatozoon is known.

obtained from the analysis of this striking variation were optimized (Fig. 10) on the topology of Faivovich et al. (2012). In that study, designed to test the monophyly of *Pleurodema*, nor Leptodactylidae neither Leiuperinae were recovered as monophyletic. However, it should be noticed that

recent phylogenetic hypotheses (Fouquet et al. 2014; Pyron 2014: Supp.Data)—with different objectives and taxonomic samplings—recovered the monophyly of both Leptodactylidae and Leiuperinae. As these two studies did not include the complete taxon sampling of *Pleurodema* included by Faivovich et al. (2012), we present the optimizations based on the latter's results. Differences in the topology for outgroups are not relevant for our inferences.

In this study the absence of axial fiber in the middle region of the tail optimizes as a synapomorphy of the leiuperinae clade formed by *Edalorhina*, *Engystomops*, *Physalaemus*, and *Pleurodema* (character 5: 0). However, due to striking variation observed in our results it is necessary to extend the studies in the other genres. None of the characters defined above optimizes as a synapomorphy of *Pleurodema*.

The acrosome complex of the spermatozoa in most species of *Pleurodema* is formed by a subacrosomal cone below the acrosome vesicle, similarly to that observed in most studied hyloid frogs. This configuration was observed in Batrachylidae (Pugin and Garrido, 1981), Bufonidae (Burgos and Fawcett, 1956; Rastogi et al., 1988; Lee and Jamieson, 1993; Meyer et al., 1997; Báo et al., 2001), Calyptocephalellidae (Pugin and Garrido, 1981), Dendrobatidae (Garda et al., 2002; Aguiar-Jr et al., 2003, 2004; Veiga-Menoncello et al., 2006, 2007), Hylidae (Rastogi et al., 1988; Lee and Kwon, 1992; Lee and Jamieson, 1993; Costa et al., 2004a,b), other Leptodactylidae (Amaral et al., 1999, 2000; Scheltinga, 2002; Zieri et al., 2008; Santos et al., 2015), Microhylidae (Scheltinga et al., 2002b), Myobatrachidae (Lee and Jamieson, 1992), and Rhinodermatidae (Pugin and Garrido, 1981). The subacrosomal cone was also observed in Ascaphidae (Jamieson et al., 1993), Leiopelmatidae (Scheltinga et al., 2001), Pelodytidae (Pugin-Ríos, 1980), Megophryidae, and Pelobatidae (Scheltinga, 2002). Furthermore, it has been reported in urodeles (Picheral, 1979; Jamieson, 1999; Scheltinga, 2002), and basal amniotes (Healy and Jamieson, 1992; Jamieson and Healy, 1992). Conversely, the subacrosomal cone is absent in some basal anuran families such as Alytidae (Furieri, 1975a), Bombinatoridae (Furieri, 1975a,b; Pugin-Ríos, 1980), Pipidae (Reed and Stanley, 1972; Bernardini et al., 1986) and Scaphiopodidae (*Scaphiopus*, James, 1970; Morrisett, 1974), and the studied victoranuran ranoid families (*sensu* Frost et al., 2006), as Dicroglossidae, Mantellidae, Phrynobatrachidae, Ptychadenidae (Scheltinga, 2002), Ranidae (Poirier and Spink, 1971; Pugin-Ríos, 1980; Scheltinga, 2002), and Rhacophoridae (Mainoya, 1981; Mizuhira et al., 1986; Muto and Kubota, 2011, 2013). As we pointed out in the description of character 0, both the definition and homology of the subacrosomal cone and conical perforatorium have been largely discussed (e.g., Lee and Jamieson, 1992, Jamieson et al., 1993; Scheltinga et al., 2001; Garda et al. 2002; Scheltinga, 2002). Although we tentatively followed the arguments of Garda et al. (2002), further studies on structure and taxonomic distribution could provide valuable information to elucidate the origin and homology of the subacrosomal cone.

In relation to *Pleurodema*, a subacrosomal cone (character 0: 2) occurs in most of its species, where this structure forms a discontinuous ring in transverse section, with the exception of *P. guayapae* and *P. marmoratum* where it is continuous. On the other hand, the subacrosomal cone of *P. bufoninum* is reduced (character 0: 1). Within hyloids, the subacrosomal cone has been considered reduced in *Lysapsus laevis* (Hylidae; Garda et al., 2004), and absent (character 0: 0) in *Pleurodema thaul* (Pugin and Garrido, 1981), *Calyptocephalella gayi* (as *Caudiverbera caudiverbera*, Calyptocephalellidae; Pugin-Ríos, 1980; Pugin and Garrido, 1981), *Leptodactylus wagneri* (Leptodactylidae; Scheltinga, 2002), *Lithodytes lineatus* and many other species of *Leptodactylus* (Leptodactylidae; Salles et al., 2015).

Transverse striations observed at midpiece (character 1: 1) in *Pleurodema guayapae* were considered in this study as homologous to those described in all *Physalaemus* species studied at present (*P. biligonigerus*, *P. gracilis*, *P. marmoratus*, and *P. nattereri*) and in some *Pseudopaludicola* species (*P. ameghini*, *P. canga*, *P. falcipes*, and *P. saltica*; Amaral et al., 1999, 2000; Zieri et al., 2008; Santos et al., 2015).

A mitochondrial collar present at the anterior portion of the tail (character 2: 1) is shared by Batrachylidae, Bufonidae, Centrolenidae, Dendrobatidae, Hylidae, Leptodactylidae, Microhylidae, and Rhinodermatidae (Pugin-Ríos, 1980; Pugin and Garrido, 1981; Jamieson et al., 1993; Lee and Jamieson, 1993; Meyer et al., 1997; Garda et al., 2002; Scheltinga et al., 2002b; Aguiar-Jr et al., 2003, 2004; Veiga-Menoncello et al., 2007; Santos et al., 2015), with the exception of a few species. The mitochondrial collar is absent in urodeles, gymnophionans, most of the basal anuran clades, the anomocoelan families, Ptychadenidae and the victoranuran families examined, including Ranidae, and Dicroglossidae, Mantellidae, Phrynobatrachidae, and Rhacophoridae (Poirier and Spink, 1971; Pugin-Ríos, 1980; Mainoya, 1981; Mizuhira et al., 1986; Scheltinga 2002; Muto and Kubota, 2011, 2013). Formerly, a well-developed mitochondrial collar, but often transient, was considered a synapomorphic condition of "Bufonoidea" (myobatrachids, leptodactylids, hylids, and bufonids; Lee and Jamieson, 1993). The taxonomic distribution of the mitochondrial collar needs to be assessed in Sooglossidae, Heleophrynidae, Nasikabatrachidae, Arthroleptidae, Hemisotidae, and Brevicipitidae in

order to establish with more certainty the transformations of this structure in the evolutionary history of anurans.

The presence of a mitochondrial collar is not constant in *Pleurodema*, while it has been observed in *P. borellii*, *P. bufoninum*, *P. cinereum*, *P. diplolister*, *P. guayapae*, and *P. marmoratum*, it is absent in *P. thaul* (Pugin and Garrido, 1981), *P. brachyops*, *P. cordobae*, *P. kriegi*, and *P. tucumanum*. However, the degeneration and loss of the mitochondrial collar is a process that is thought to occur late in spermiogenesis (Garrido et al., 1989); therefore, the characteristics of the midpiece could be variable along spermatogenesis.

The ultrastructural features of the spermatozoid tail of the studied species of *Pleurodema* are also noticeably variable. In most hyloids, the typical tail arrangement includes an axoneme and evident accessory fibers (juxtaxonemal fiber + axial fiber) separated by a thin undulating membrane (Scheltinga, 2002; Costa et al., 2004a, as "Bufonoidea"). In *Pleurodema*, a striking variety of arrangements have been observed in the tail morphology. In *P. brachyops*, *P. cordobae*, *P. diplolister*, *P. kriegi*, *P. guayapae*, and *P. marmoratum* the medial region of the tail shows a juxtaxonemal fiber and an undulating membrane, while the axial fiber is absent, as it occurs in the studied species of *Physalaemus* (characters 4: 1, 5: 0; Amaral et al., 1999; Zieri et al., 2008). Within the studied species of Leptodactylidae, the axial fiber and juxtaxonemal fiber separated by thin undulating membrane are known so far in *Pseudopaludicola ameghini*, *P. falcipes*, *P. mineira*, *P. saltica*, and *P. ternetzi* (Amaral et al., 2000; Santos et al., 2015), *Leptodactylus wagneri* (Scheltinga, 2002), *Leptodactylus bufonius*, *L. chaquensis*, *L. furnarius*, *L. fuscus*, *L. labyrinthicus*, *L. latinasus*, *L. latrans*, *L. paraensis*, *L. petersii*, *L. podicipinus, L. syphax*, and *Lithodytes lineatus* (Salles et al., 2015). Moreover, *Pleurodema thaul* and *Engystomops pustulosus* are the only species of leiuperines so far known with abaxonemal bulb-like swelling distally to the paraxonemal rod (character 7: 1), described and interpreted as the axial fiber by Pugin and Garrido (1981) and Scheltinga (2002), respectively.

Several independent losses of the undulating membrane and accessory fibers took place during the evolutionary history of anurans. *Pleurodema bufoninum* and *P. thaul* are characterized by the presence of a paraxonemal rod (character 6: 1), and the absence of undulating membrane (character 8: 0). The tail in the clade *P. tucumanum* + (*P. borellii* + *P. cinereum*) is characterized by the absence of both juxtaxonemal fiber (character 4: 0) and undulating membrane (character 8: 0). Also, the occurrence of a cytoplasmatic sheath surrounding the axoneme (character 3: 1) shared by *P. borellii* and *P. cinereum* is an apomorphic character not observed in other species (Fig. 7F–H). On the other hand, *P. tucumanum* has a simple tail formed only by an axoneme. These specific arrangements of the tail of *P. borellii*, *P. cinereum*, and *P. tucumanum* have not been described for other leptodactylids. The simple tail occurs in ranoids and some basal anurans (see Lee and Jamieson, 1993 and reference therein) while in hyloids, this type of tail has only been described in the hylids *Lysapsus* and *Pseudis* (Garda et al., 2004), and the telmatobiid *Telmatobius* sp. (Pisanó and Adler, 1968; Scheltinga, 2002).

## Implications of Sperm Ultrastructure in the Fertilization Environment

Some studies in lissamphibians have suggested that external fertilization is primitive, and that internal fertilization has been acquired independently in the three orders (e.g. Boisseau and Joly 1975; Hecht and Edwards 1976; Duellman and Trueb, 1994), as corroborated by our current knowledge in phylogenetic relationships of amphibians (Pyron and Wiens, 2011). Lee and Jamieson (1993) proposed that complex sperm occurs in species with internal fertilization, as caecilians, salamandroid urodeles, and a basal anuran (e.g. *Ascaphus truei*; Jamieson et al., 1993). Anurans with a highly viscous fertilization environment (e.g. internal fertilization, foam-nests) tend to have spermatozoa that have been considered a more complex structure than those with a low-viscosity fertilization environment (e.g., fresh water; see Muto and Kubota, 2013 and reference herein). The absence of accessory fibers and an undulating membrane was postulated as characteristic in anurans with external fertilization on water (e.g., Jamieson et al., 1993; Lee and Jamieson, 1993; Garda et al., 2004). While these release their sperm and ova in water, where fertilization occurs, most Leiuperinae release their gametes in a viscous environment, the foam-nest. Differences in sperm morphology are thought to have evolved as a result of selective pressure from the fertilization environment (Jamieson et al., 1993; Lee and Jamieson, 1993).

Previous studies on the spermatozoa of foam-making rhacophorids showed that some species share certain complex morphological features that offset the viscous resistance of the foam. Characters such as a pair of axonemes and crystallized satellite microtubules were found in the thick tail of *Polypedates leucomystax* (Muto and Kubota, 2013), and provide more propulsion power than a single axoneme and flagellar stiffness. In addition, a corkscrew-shaped head is present in *Chiromantis xerampelina* (Mainoya, 1981), *Rhacophorus schlegelli* and *R. arboreus* (Mizuhira et al., 1986; Muto and Kubota 2009), which facilitates the penetration of the viscous foam-nest (Wilson et al., 1991, Muto and Kubota, 2009, 2013). Muto and

Kubota (2009, 2013) showed that the arrangement of two axonemes is critical for the motility of spermatozoa in rhacophorids and that the frequency of beating of the sperm tail was increased in high-viscosity solution. Similarly, these authors found that nonfoam-nesting rhacophorid (*Buergeria buergeri*) do not exhibit complex features, but rather have a single axoneme in the tail as do the taxa that release their gametes in water (Muto and Kubota, 2013). Other foam-nesting species such as limnodynastids [*Adelotus brevis* (Lee and Jamieson, 1993), *Limnodynastes* sp. (Lee and Jamieson, 1992; Scheltinga, 2002), and *Heleiphorus albopunctatus* (Scheltinga, 2002)] and many leptodactylids (Scheltinga, 2002; Salles et al., 2015) were studied. All these species have a tail with accessory fibers and undulating membrane. In conclusion, all these spermatozoa morphologies (i.e., the corkscrew-shaped head, the arrangement of axonemes, the crystallized satellite microtubules, the tail with accessory fibers and undulating membrane) do achieve the fertilization in this viscous environment. In addition, Salles et al. (2015) suggested that structures as the acrosome and nuclear complex may be associated with the occurrence of polyandrous mating in species of the Leptodactylinae.

The foam-making species included in the phylogenetic hypothesis of Faivovich et al. (2012) are shown with a red square in Figure 10. All foam-making Leiuperinae, for which spermatozoa are known, lack an axial fiber. Also, *Pleurodema borellii* and *P. cinereum* share a cytoplasmatic sheath surrounding the axoneme, while *P. tucumanum* has no accessory fibers associated to the axoneme. Muto and Kubota (2013) showed that spermatozoa of *Buergeria buergeri* in high-viscosity solutions are propelled straight forward but the cruising speed was clearly reduced. So probably there is a range of viscous environments in where the sperm can move. The spermatozoa of *P. borellii*, *P. cinereum*, and *P. tucumanum* successfully move forward in a viscous environment and achieve fertilization of the egg, but whether this is at the expense of changes in the movement speed should be tested experimentally. By way of counteract the opposition of the environment, both the cytoplasmatic sheath (*P. borellii* and *P. cinereum*) and the amount of mitochondria surrounding the axoneme (*P. tucumanum*) may be associated with the necessity of swimming in a viscous medium fertilization.

The study of spermatozoid morphology in *Pleurodema* showed that the acrosome complex, the mitochondrial collar, and the tail have variable arrangements. The optimization of the characters presented in the present paper should be reconsidered when a phylogenetic hypothesis of leiuperines is available. Conversely, sperm morphology in *Pleurodema* did not reveal any evident association with fertilization in a viscous environment. Knowledge on spermatozoid morphological diversity in other leptodactylids is still too sparse to understand if the diversity that we find in foam fertilizing species occurs as well in the other foam nesters of the family.

## APPENDIX

• • •

Examined specimens are housed in the following institutions: Museo de La Plata (MLP A., La Plata, Argentina), Museo Argentino de Ciencias Naturales "Bernardino Rivadavia" (MACN, Buenos Aires, Argentina), Centro Nacional de Investigaciones Iológicas (CENAI, housed at MACN), Laboratorio de Genética Evolutiva, Instituto de Biología Subtropical CONICET-UNaM (LGE, Misiones, Argentina), and Museu de Zoologia Prof. Adão J. Cardoso, Instituto de Biologia Unicamp (ZUEC, Campinas, Brazil).

*Pleurodema borellii*. MACN 42027. ARGENTINA: Catamarca: Ambato: Ruta Provincial N° 1 and Río Suinguil.

*Pleurodema brachyops*. CENAI 8781. PANAMA: Nueva Gorgona.

*Pleurodema bufoninum*. MACN 38299. ARGENTINA: Río Negro: Pilcaniyeu: Ruta N° 80 and Arroyo Las Bayas.

*Pleurodema cinereum*. MLP A. 4689. ARGENTINA: Jujuy: Tilcara: Juella.

*Pleurodema cordobae*. MACN 40549. ARGENTINA: Córdoba: Estancia Los Tabaquillos.

*Pleurodema diplolister*. ZUEC 12367–12368. BRAZIL: Maranhão: Barreirinhas: Vassouras.

*Pleurodema guayapae*. MACN 48398–49399. ARGENTINA: San Luis: Ayacucho: Ruta Provincial N° 79, 11 km N Candelaria.

*Pleurodema kriegi*. CENAI 3278-5. ARGENTINA: Córdoba: Pampa de Achala.

*Pleurodema marmoratum*. CENAI 10767. BOLIVIA: Tiahuanacu, 65 km North La Paz. LGE 6281. ARGENTINA: Jujuy: Tumbaya El Quemado.

*Pleurodema tucumanum*. MACN 45428. ARGENTINA: Santiago del Estero: Banda: Ruta Provincial N° 5, 7 km E crossing Ruta Nacional N° 34. MACN 48397. ARGENTINA: San Luis: Ayacucho: Ruta Provincial N° 79, 11 km N Candelaria.

## ACKNOWLEDGMENTS

The authors thank S.J. Nenda and M.O. Pereyra (MACN) for technical assistance, J. Williams (MLP) and D. Baldo (LGE) for the loan of specimens under his care, D. Baldo, B. Blotto, A. Brunetti, A. Dallagnol and J. Rajmil for their help during field work, and S. Rosset for discussing character coding. We are very grateful to the Editor and reviewers for comments and suggestions that improved our manuscript. This work was

supported by grants PICTs 2011-1524, 2011-1895, 2012-2687, 2013-404, 2014-2035; CONICET PIP 11220110100889; UBACyT 2012–2014 20020110200213; and 2015-2017 20020130100828BA; and grants # 2012/10000-5, # 2013/50741-7 and # 2013/04076-1 São Paulo Research Foundation (FAPESP).

## LITERATURE CITED

Aguiar- Jr O, Garda AA, Lima AP, Colli GR, Báo SN, Recco-Pimentel SM. 2003. The biflagellate spermatozoon of the dart-poison frogs *Epipedobates femoralis* and *Colostethus* sp. (Anura, Dendrobatidae). J Morphol 255:114–121.

Aguiar-Jr O, Lima AP, Báo SN, Recco-Pimentel SM. 2004. Sperm ultrastructure of the Brazilian Amazon poison frogs *Epipedobates trivittatus* and *Epipedobates hahneli* (Anura, Dendrobatidae). Acta Zool 85:21–28.

Aguiar-Jr O, Giaretta AA, Recco-Pimentel SM. 2006. The sperm of Hylodinae species (Anura, Leptodactylidae): Ultrastructural characteristics and their relevance to interspecific taxonomic relationships. J Bioscience 31:379–388.

Amaral MJLV, Fernandes AP, Báo SN, Recco-Pimentel SM. 1999. An ultrastructural study of spermiogenesis in three species of *Physalaemus* (Anura, Leptodactylidae). Biocell 23: 211–221.

Amaral MJLV, Fernandes AP, Báo SN, Recco-Pimentel SM. 2000. The ultrastructure of spermatozoa in *Pseudopaludicola falcipes* (Anura, Leptodactylidae). Amphib Reptil 21:498–502.

Báo SN, Dalton GC, Oliveira SF. 1991. Spermiogenesis in *Odontophrynus cultripes* (Amphibia, Anura, Leptodactylidae): Ultrastructural and cytochemical studies of proteins using E-PTA. J Morphol 207:303–314.

Báo SN, Vieira GH, Fernandes AP. 2001. Spermiogenesis in *Melanophryniscus cambaraensis* (Amphibia, Anura, Bufonidae): Ultrastructural and cytochemical studies of carbohydrates using lectins. Cytobois 106:203–216.

Barrio A. 1954. Contribución a la etología y reproducción del batracio *Pseudopaludicola falcipes*. Rev Arg Zoogeografía 5: 37–43.

Barrio A. 1964. Especies crípticas del genero *Pleurodema* que conviven en una misma área identificadas por el canto nupcial (Anura, Leptodactylidae). Physis 24:471–489.

Barrio A. 1977. Aportes para la elucidación del "status" taxonómico de *Pleurodema bibroni* Tschudi y *Pleurodema kriegi* (Müller) (Amphibia, Anura, Leptodactylidae). Physis 37:311–331.

Bernardini G, Stipani R, Melone G. 1986. The ultrastructure of *Xenopus* spermatozoon. J Ultrastruct Mol Struct Res 94:188–194.

Boisseau C, Joly T. 1975. Transport and survival of spermatozoa in female Amphibia. In: Hafez ESE, Thibault CG, editors. The Biology of Spermatozoa: Transport, Survival and Fertilizing Ability. Basel: Karger. pp 94–104.

Burgos MH, Fawcett DW. 1956. An electron microscope study of spermatid differentiation in the toad, *Bufo arenarum* Hensel. J Biophys Biochem Cytol 2:223–239.

Cei JM. 1962. Batracios de Chile. Santiago, Chile: Ediciones Universidad de Chile. 128p.

Cei JM. 1980. Amphibians of Argentina. Monitore Zool Ital (NS) Monogr 2:1–609.

Costa GC, Vieira GHC, Teixeira RD, Garda AA, Colli GR, Báo SN. 2004a. An ultrastructural comparative study of the sperm of *Hyla pseudopseudis*, *Scinax rostratus*, and *S. squalirostris* (Amphibia: Anura: Hylidae). Zoomorph 123:191–197.

Costa GC, Garda AA, Teixeira RD, Colli GR, Báo SN. 2004b. Comparative analysis of the sperm ultrastructure of three species of *Phyllomedusa* (Anura, Hylidae). Acta Zool (Stockh) 85:257–262.

Duellman WE, Trueb L. 1994. Biology of Amphibians. Baltimore: The Johns Hopkins University Press. 670 p.

Duellman WE, Veloso A. 1977. Phylogeny of *Pleurodema* (Anura: Leptodactylidae): A biogeographic model. Occas Pap Mus Nat Hist Univ Kansas 64:1–46.

Faivovich J, Ferraro DP, Basso NG, Haddad CFB, Rodrigues MT, Wheeler WC, Lavilla EO. 2012. A phylogenetic analysis of *Pleurodema* (Anura: Leptodactylidae: Leiuperinae) based on mitochondrial and nuclear gene sequences, with comments on the evolution of anuran foam nests. Cladistics 28:460–482.

Ferraro DP, Pereyra ME, Baldo JD, Faivovich J. 2016. The clutch structure of *Pleurodema tucumanum* (Anura: Leptodactylidae). Salamandra 52:48–52.

Fouquet A, Cassini C, Haddad CFB, Pech N, Rodrigues MT. 2014. Species delimitation, patterns of diversification and historical biogeography of a Neotropical frog genus *Adenomera* (Anura, Leptodactylidae). J Biogeogr 41:855–870.

Frost, DR. 2015. Amphibian Species of the World: An Online Reference. Version 6.0 (July 17, 2015). Electronic Database Available at http://research.amnh.org/herpetology/amphibia/index.html. American Museum of Natural History, New York.

Frost DR, Grant T, Faivovich J, Bain RH, Haas A, Haddad CFB, De Sá RO, Channing A, Wilkinson M, Donnellan SC, Raxworthy CJ, Campbell JA, Blotto BL, Moler P, Drewes RC, Nussbaum RA, Lynch JD, Green DM, Wheeler WC. 2006. The amphibian tree of life. Bull Am Mus Nat Hist 297:1–370.

Furieri P. 1975a. La morfologia comparata degli spermi di *Discoglossus pictus* Otth., *Bombina variegata* (L.) e *Alytes obstetricans* (Laurenti). Boll Zool 42:458–459.

Furieri P. 1975b. The peculiar morphology of the spermatozoon of *Bombina variegata* (L.). Monit Zool Ital 9:185–201.

Garda AA, Colli GC, Aguiar-Jr O, Recco-Pimentel SM, Báo SN. 2002. The ultrastructure of the spermatozoa of *Epipedobates flavopictus* (Amphibia, Anura, Dendrobatidae), with comments on its evolutionay significance. Tissue Cell 34:356–364.

Garda AA, Costa GC, Colli GR, Báo SN. 2004. Spermatozoa of Pseudinae (Amphibia, Anura, Hylidae), with a test of the hypothesis that sperm ultrastructure correlates with reproductive modes in anurans. J Morphol 261:196–205.

Garrido O, Pugin E, Jorquera B. 1989. Sperm morphology of *Batrachyla* (Anura: Leptodactylidae). Amphib Reptil 10:141–149.

Giaretta AA, Facure KG. 2009. Habitat, egg-laying behaviour, eggs and tadpoles of four sympatric species of *Pseudopaludicola* (Anura, Leiuperidae). J Nat Hist 43:995–1009.

Healy JM, Jamieson BGM. 1992. Sperm ultrastructure in the tuatara (*Sphenodon punctatus*) and its relevance to the relationships of the Sphenodontida. Philos Trans R Soc Lond 335: 193–205.

Hecht MK, Edwards JL. 1976. The methodology of phylogenetic inference above the species level. In: Hecht MK, Goody PC, Hecht BM, editors. Major Patterns in Vertebrate Evolution. London: Plenum. pp 3–51.

Hödl W. 1992. Reproductive behaviour in the Neotropical foam-nesting frog *Pleurodema diplolistris* (Leptodactylidae). Amphib Reptil 13:263–274.

James WS. 1970. The ultrastructure of anuran spermatids and spermatozoa [dissertation]. University of Tennessee. 121p.

Jamieson BGM. 1999. Spermatozoal phylogeny of the Vertebrata. In: Gagnon C, editor. The Male Gamete: From Basic Science to Clinical Applications. Vienna: Cache River Press. pp 303–331.

Jamieson BGM, Healy JM. 1992. The phylogenetic position of the tuatara. *Sphenodon punctatus* (Sphenodontida, Amniota) as indicated by a cladistic analysis of the ultrastructure of spermatozoa. Philos Trans R Soc Lond 335:207–219.

Jamieson BGM, Lee MSY, Long K. 1993. Ultrastructure of the spermatozoon of the internally fertilizing frog *Ascaphus truei* (Ascaphidae: Anura: Amphibia) with phylogenetic considerations. Herpetologica 49:52–65.

Lee MSY, Jamieson BGM. 1992. The ultrastructure of the spermatozoa of three species of myobatrachid frogs (Anura, Amphibia) with phylogenetic considerations. Acta Zool (Stockh) 73:213–222.

Lee MSY, Jamieson BGM. 1993. The ultrastructure of the spermatozoa of bufonid and hylid frogs (Anura, Amphibia): Implications for phylogeny and fertilization biology. Zool Scr 22: 309–323.

Lee YH, Kwon AS. 1992. Ultrastructure of spermiogenesis in *Hyla japonica* (Anura, Amphibia). Acta Zool (Stockh) 73:49–55.

Mainoya JR. 1981. Observations on the ultrastructure of spermatids in the testis of *Chiromantis xerampelina* (Anura: Rhacophoridae). Afr J Ecol 19:365–368.

Martori R, Aún L, Vignolo PE. 1994. Aporte al conocimiento de la biología y distribución de *Pleurodema tucumana* (Anura, Leptodactylidae). Bol Asoc Herpetol Arg 10:18–19.

Meyer E, Jamieson BGM, Scheltinga DM. 1997. Sperm ultrastructure of six Australian hylid frogs from two genera (*Litoria* and *Cyclorana*): Phylogenetic implications. J Submicrosc Cytol Pathol 29:443–451.

Mizuhira V, Futaesaku Y, Ono M, Ueno M, Yokofujita J, Oka T. 1986. The fine structure of the spermatozoa of two species of *Rhacophorus* (*arboreus*, *schlegelii*). I. Phase-contrast microscope, scanning electron microscope, and cytochemical observations of the head piece. J Ultrastruct Mol Struct Res 96: 41–53.

Morrisett FW. 1974. Comparative ultrastructure of sperm in three families of Anura (Amphibia) [dissertation]. Arizona State University. 56p.

Muto K, Kubota HY. 2009. A novel mechanism of sperm motility in a viscous environment: Corkscrew-shaped spermatozoa cruise by spinning. Cell Motil Cytoskel 66:281–291.

Muto K, Kubota HY. 2011. Ultrastructural analysis of spermiogenesis in *Rhacophorus arboreus* (Amphibia, Anura, Rhacophoridae). J Morphol 272:1422–1434.

Muto K, Kubota HY. 2013. Ultrastructure and motility of the spermatozoa of *Polypedates leucomystax* (Amphibia, Anura, Rhacophoridae). Cytoskeleton 70:121–133.

Nixon, KC. 2002. WinClada, vers. 1.00.8. Nixon, Ithaca, NY.

Picheral B. 1979. Structural, comparative, and functional aspects of spermatozoa in urodeles. In Fawcett DW, Bedford JM, editors. The Spermatozoon. Baltimore: Urban and Schwarzenberg. pp 267–287.

Pisanó A, Adler R. 1968. Submicroscopical aspects of *Telmatobius hauthali schreiteri* spermatids. Z Zellforsch Mikrosk Anat 87:345–349.

Poirier GR, Spink GC. 1971. The ultrastructure of testicular spermatozoa in two species of *Rana*. J Ultrastruct Res 36: 455–465.

Pugin-Ríos E. 1980. Étude comparative sur la structure du spermatozoïde des amphibiens anoures. Comportement des gamètes lors de la fécondation [Dissertation]. L'Université de Rennes. 114p.

Pugin E, Garrido O. 1981. Morfología espermática en algunas especies de anuros pertenecientes al bosque temperado del sur de Chile. Ultraestructura comparada. Medio Ambiente 5: 47–57.

Pyron RA. 2014. Biogeographic analysis of amphibians reveals both ancient continental vicariance and recent oceanic dispersal. Syst Biol 63:779–797.

Pyron RA, Wiens JJ. 2011. A large-scale phylogeny of Amphibia including over 2800 species, and a revised classification of extant frogs, salamanders, and caecilians. Mol Phylogenet Evol 61:543–583.

Rastogi RK, Bagnara JT, Iela L, Krasovich MA. 1988. Reproduction in the Mexican leaf frog, *Pachymedusa dacnicolor*. IV. Spermatogenesis: A light and ultrasonic study. J Morphol 197:277–302.

Reed SC, Stanley HP. 1972. Fine structure of spermatogenesis in the South African clawed toad *Xenopus laevis* Daudin. J Ultrastruct Res 41:277–295.

Reynolds ES. 1963. The use of lead citrate at high pH as an electron opaque stain in electron microscopy. J Cell Biol 17: 208–212.

Salles NME, Zara FJ, Prado CPA. 2015. Differences in sperm morphology in foam-nesting leptodactyline frogs (Anura, Leptodactylidae. Acta Zool. (Stockholm) doi:10.1111/azo.12144.

Santos JS, Introíni GO, Veiga-Menoncello ACP, Recco-Pimentel SM. 2015. Ultrastructure variation in the spermatozoa of *Pseudopaludicola* frogs (Amphibia, Anura, Leptodactylidae), with brief comments on its phylogenetic relevance. J Morphol 276:1495–1504.

Scheltinga DM. 2002. Ultrastructure of spermatozoa of the Amphibia: Phylogenetic and taxonomic implications [Dissertation]. University of Queensland. 374p.

Scheltinga DM, Jamieson BGM. 2003. Spermatogenesis and the mature spermatozoon: Form, function and phylogenetic implications. In: Jamieson BGM, editor. Reproductive Biology and Phylogeny of Anura. New Hampshire: Science Publishers. pp 119–252.

Scheltinga DM, Jamieson BGM, Eggers KE, Green DM. 2001. Ultrastructure of the spermatozoon of *Leiopelma hochstetteri* (Amphibia, Anura, Leiopelmatidae). Zoosystema 23:157–171.

Scheltinga DM, Jamieson BGM, McDonald KR. 2002a. Ultrastructure of the spermatozoa of *Litoria longirostris* (Hylidae, Anura, Amphibia): Modifications for penetration of a gelatinous layer surrounding the arboreal egg clutch. Mem Queensl Mus 48:215–220.

Scheltinga DM, Jamieson BGM, Bickford DP, Garda AA, Báo SN, McDonald KR. 2002b. Morphology of the spermatozoa of the Microhylidae (Anura, Amphibia). Acta Zool (Stockh) 83: 263–275.

Veiga-Menoncello ACP, Lima AP, Recco-Pimentel SM. 2006. Sperm morphology of five species of *Colostethus* (Anura, Dendrobatidae) from Brazil, with phylogenetic comments. Acta Zool 87:147–157.

Veiga-Menoncello ACP, Aguiar- Jr O, Lima AP, Recco-Pimentel SM. 2007. The biflagellate spermatozoa of *Colostethus marchesianus* (Melin, 1941) (Anura, Dendrobatidae) from the type locality and of *Colostethus* sp. (aff. Marchesianus.) from a different locality: A scanning and transmission electron microscopy analysis. Zool Anz 246:46–59.

Weigandt M, Úbeda CA, Diaz M. 2004. The larva of *Pleurodema bufoninum* Bell, 1843, with comments on its biology and on the egg strings (Anura, Leptodactylidae). Amphib Reptil 25:429–437.

Wilson BA, Van Der Horst G, Channing A. 1991. Scanning electron microscopy of the unique sperm of *Chiromantis xerampelina* (Amphibia: Anura). Electron Microsc Soc S Afr 21:255–256.

Zieri R, Taboga SR, Oliveira C. 2008. Espermiogênese em *Eupemphix nattereri* (Anura, Leiuperidae): Aspectos ultraestruturais. Iheringia 98:193–199.